Hybrid Advances 7 (2024) 100305

Contents lists available at ScienceDirect

Hybrid Advances

journal homepage: www.journals.elsevier.com/hybrid-advances

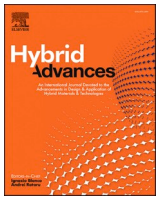

Research Article

Analytical investigation of green composite lamina utilizing natural fiber to strengthen PLA

B. Vishwash [a,*], N.D. Shivakumar [a], K.B. Sachidananda [b]

[a] Department of Design and Manufacturing, Indian Institute of Science, CV Raman Rd, Bengaluru, Karnataka, 560012, India
[b] Department of Mechanical Engineering, Sri Krishna Institute of Technology, Bangalore, Karnataka, 560090, India

ARTICLE INFO

Keywords:
Polylactic acid (PLA)
Natural fiber reinforced green composites (NFRGCs)
Bamboo
Flax
Jute
Fiber volume fraction and engineering constants

ABSTRACT

This work's main goal is to investigate the effects of the natural fiber orientation angle on the lamina's engineering constants, such as the shear modulus, major Poisson's ratio, longitudinal and transverse Young's moduli, and lamina level shear coupling coefficients. The PLA matrix of the three green composite laminas under study is reinforced with natural fiber. The three natural fibers under study are flax, jute, and bamboo fibers. The study assesses the performance of three PLA laminas reinforced with natural fibers for each of the previously listed engineering constants. The behavior of the green composite lamina for various fiber volume fractions is also presented in this study. This analytical investigation employs the macromechanics of lamina to do the examination. The investigation's findings demonstrated that the volume % and fiber orientation have a considerable impact on the lamina's engineering constants. The study offers a comprehensive variation of the lamina's engineering constants for each fiber orientation angle between 0 and 90° and for each fiber volume fraction between 0 % (entirely matrix) and 100 % (completely fibers) in steps of 5 %. The outcomes of the presented study will help in the design of the facesheets for the composite sandwich structures. The results presented can be used to check the viability of using natural fibers to strengthen different polymer matrices. Bamboo-PLA lamina outperforms flax-PLA and jut-PLA laminae.

1. Introduction

Natural fibers and a biodegradable polymer matrix combine to form green composites, sometimes referred to as biocomposites. These materials are designed to be eco-friendly substitutes for conventional composites. Types of natural fibers include flax, hemp, jute, kenaf, sisal, coir, bamboo, etc. and several biodegradable polymer kinds, including polylactic acid (PLA), polyhydroxyalkanoates (PHA), and starch-based polymers [1,2]. Green composites typically exhibit good tensile strength, based on the kind of matrix and fiber utilized. Natural fibers provide good stiffness, enhancing the rigidity of the composite [3]. Impact resistance of green composite is generally lower than synthetic composites however they can be enhanced with the right fiber modifications and composite design [4]. Green composites have moderate thermal stability, influenced by the kind of polymer matrix and fiber. Natural fibers have low thermal conductivity, making green composites good insulators [5,6]. Among the primary benefits of green composites is their ability to biodegrade, reducing environmental impact [7,8]. Green composites face challenges like moisture absorption [9,10], fiber-matrix adhesion and standardization. Natural fibers tend to collect humidity, as this may affect the mechanical qualities and durability of the composite [11,12]. Achieving good cling between natural fibers and the matrix is challenging, affecting the overall performance of the composite [13,14]. Lack of standardized testing methods and material specifications can hinder the widespread adoption of green composites [15]. Green composites represent a promising area of materials science, offering sustainable alternatives for various industries. Continued research and development are expected to address current challenges and expand the applications of these eco-friendly materials. In this work, we have performed an analytical research on three laminas comprising the PLA-based green composite, the three natural fibers—jute, flax, and bamboo—are employed as reinforcements in the aforementioned green composite under investigation.

The thermoplastic polyester known as PLA, or polylactic acid, is made utilizing sustainable assets like starch from maize, cassava, or sugarcane. Lactic acid, a naturally occurring material, is produced when PLA hydrolyzes its ester linkages in the presence of moisture. It is extensively utilized in packaging, biodegradable goods, and 3D printing

* Corresponding author.
E-mail addresses: bbvishwash@gmail.com (B. Vishwash), shivak@iisc.ac.in (N.D. Shivakumar), sachidananda.kb@gmail.com (K.B. Sachidananda).

https://doi.org/10.1016/j.hybadv.2024.100305
Received 22 July 2024; Received in revised form 28 September 2024; Accepted 4 October 2024
Available online 11 October 2024
2773-207X/© 2024 The Authors. Published by Elsevier B.V. This is an open access article under the CC BY-NC-ND license (http://creativecommons.org/licenses/by-nc-nd/4.0/).

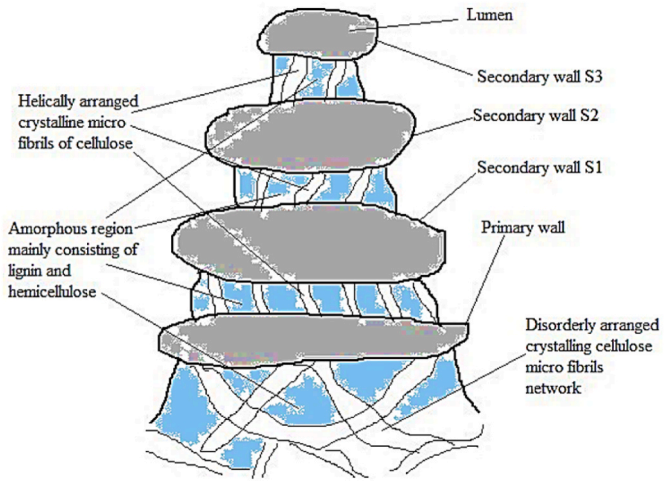

Fig. 1. Diagram showing how natural fibers are arranged structurally [25].

Table 1
Engineering constant values of natural fibers.

Natural Fibers	Young's Modulus E_f (GPa)	Poisson's Ratio ν_f	Ref.
Bamboo	17–89	0.180–0.334	[32,41,42]
Flax	27.6–103	0.34–0.498	[32,41,43,44]
Jute	10–55	0.11–0.374	[32,41,43,45, 46]

Table 2
Engineering constant values of PLA matrix.

Elastic Modulus E_m (GPa)	Poisson's Ratio ν_m	Ref.
3.565 to 4.407	0.142–0.351	[47]

[16]. Ester linkages bond lactic acid monomers together form the polymer known as PLA. Different varieties of PLA can be produced from the two stereoisomeric forms of lactic acid, L-lactic acid and D-lactic acid [17]. PLA has the following physical characteristics: a density of around 1.28 g/cm^3, a glass transition temperature of 60–65 °C, and a melting temperature of 150–160 °C [18]. Tensile strength of 52–72 MPa, elongation at break of 3–11 %, Young's modulus of 2.5–16 GPa, Poisson's ratio of 0.313–0.351, and impact strength are among the mechanical characteristics of PLA that set it apart from other plastics [17,18]. PLA starts to thermally decompose at 200 °C, while the temperature at which heat deflection occurs is between 55 and 60 °C. Under industrial composting conditions (high temperature and humidity), PLA can be composted. In ambient settings, it does not biodegrade easily [18]. PLA is preferred because it is renewable and environmentally friendly, but its mechanical and thermal stability may be a drawback for particular applications. However, these qualities can be improved by strengthening the PLA with both natural and synthetic fibers [17,18]. Using the solvent casting process, it was possible to efficiently reinforce untreated and acetylated nanocrystalline cellulose into PLA polymer, which had a beneficial effect on both tensile and Young's modulus. Additionally, the addition of acetylated nanocrystalline cellulose improved thermal stability, but the addition of untreated nanocrystalline cellulose had no discernible impact. This outcome suggests that the acetylation process has enhanced nanocrystalline cellulose's potential for use as PLA polymer reinforcing material [19]. The present paper examines the improved properties brought about by the natural fibers jute, flax, and bamboo. The details of these natural fiber are presented in next section.

Based on the macromechanics of the lamina, this work presents an analytical study that explores the effects of different fiber orientation angles at different volume fractions on the engineering constants of the lamina, such as the lamina level shear coupling coefficients, longitudinal Young's modulus, transverse Young's modulus, shear modulus, and Poisson's ratio. The lamina of the study is made of PLA matrix that has been strengthened using natural yarns. The three types of natural fibers - jute, flax, and bamboo - are investigated. The paper comprises five parts. The first part gives a summary of green composites and their importance. It also provides the framework of the paper. The three natural fibers that this paper will be examining are covered in the subsection of the second part, which discusses the anatomy of natural fibers. The third

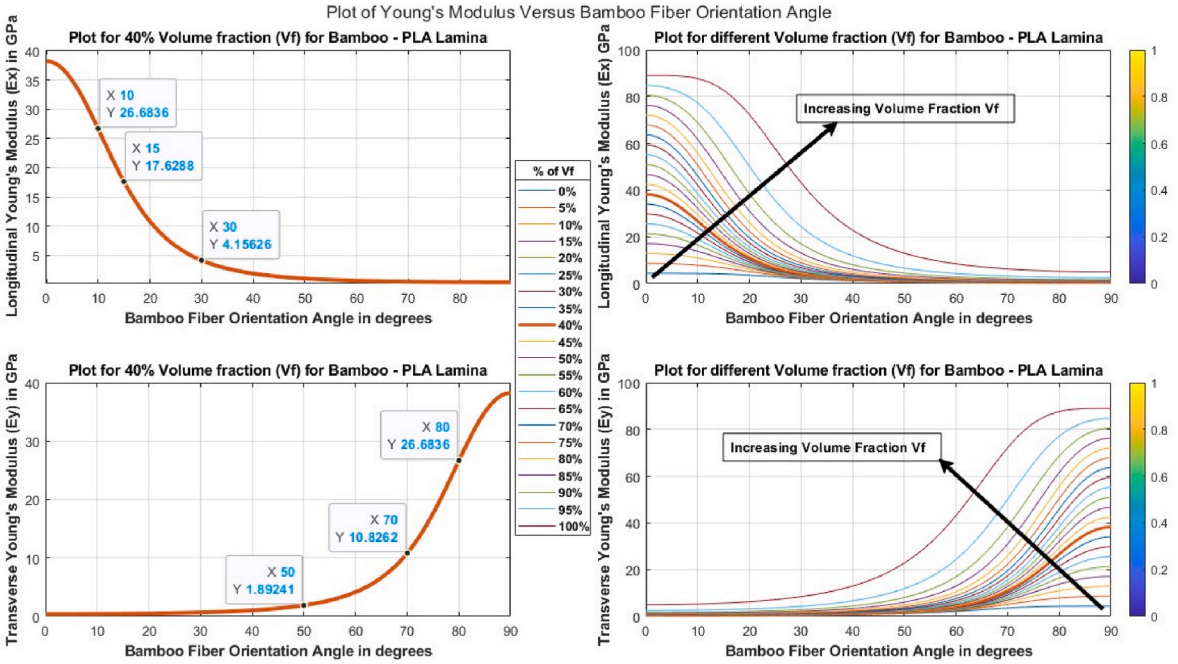

Fig. 2. Changing Young's moduli with fiber orientation for bamboo-PLA lamina.

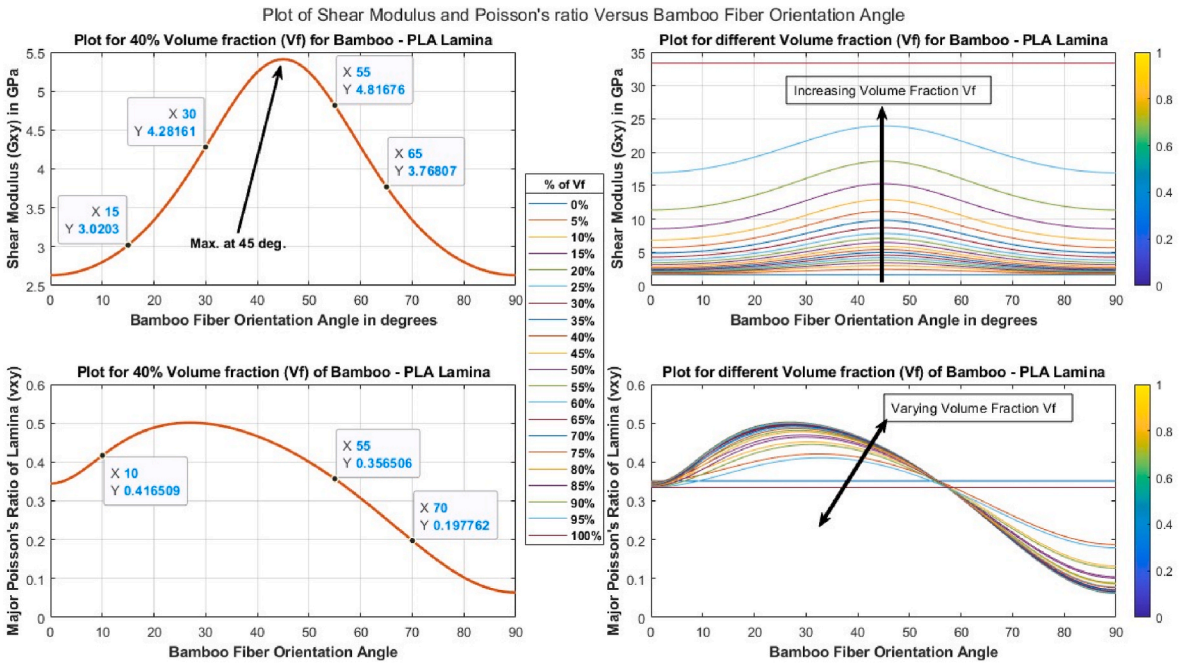

Fig. 3. Changing G_{xy} and ν_{xy} ratio with fiber orientation for bamboo-PLA lamina.

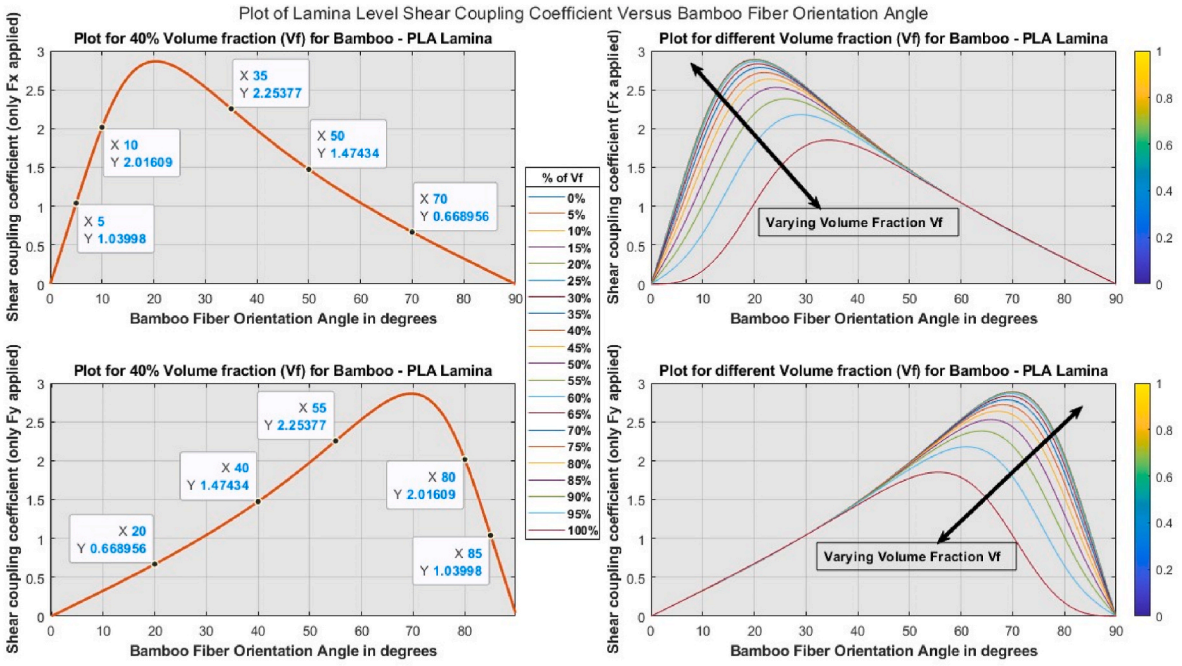

Fig. 4. Changing lamina level shear coupling coefficients with fiber orientation for bamboo-PLA lamina.

section presents the macromechanics approach used in the lamina performance study. Fourth part contains the results, final portion presents the discussion and ends with conclusion.

2. Fibers anatomy

Natural fibers consist of several layers and are hollow. The lumen, a hollow section in the heart of the plant, is used to move nutrients and water throughout the body. The lumen's size diminishes over time, making it possible to assess the fiber's maturity and quality. The primary and secondary walls are the next two layers. Since they are hollow, natural fibers typically have a polygonal cross section; however, because this section is frequently not axisymmetric, the external diameter is not accurately measured [20]. The mechanical efficiency of a fiber is considerably influenced by its diameter, since a larger diameter yields a lower tensile modulus and lower stress [21]. These fibers' hollowness has an additional impact on their mechanical qualities since it makes it difficult to determine the precise area of the natural fibers, which causes elongation strength and modulus values to be exaggerated. Because most procedures do not make use of this void, the overall permeability of a composite can also be raised by the lumen's dimension, resulting in spongy substances with considerable absorbance of wetness that aren't always preferred [22].

From a mechanical perspective, the secondary wall is the most

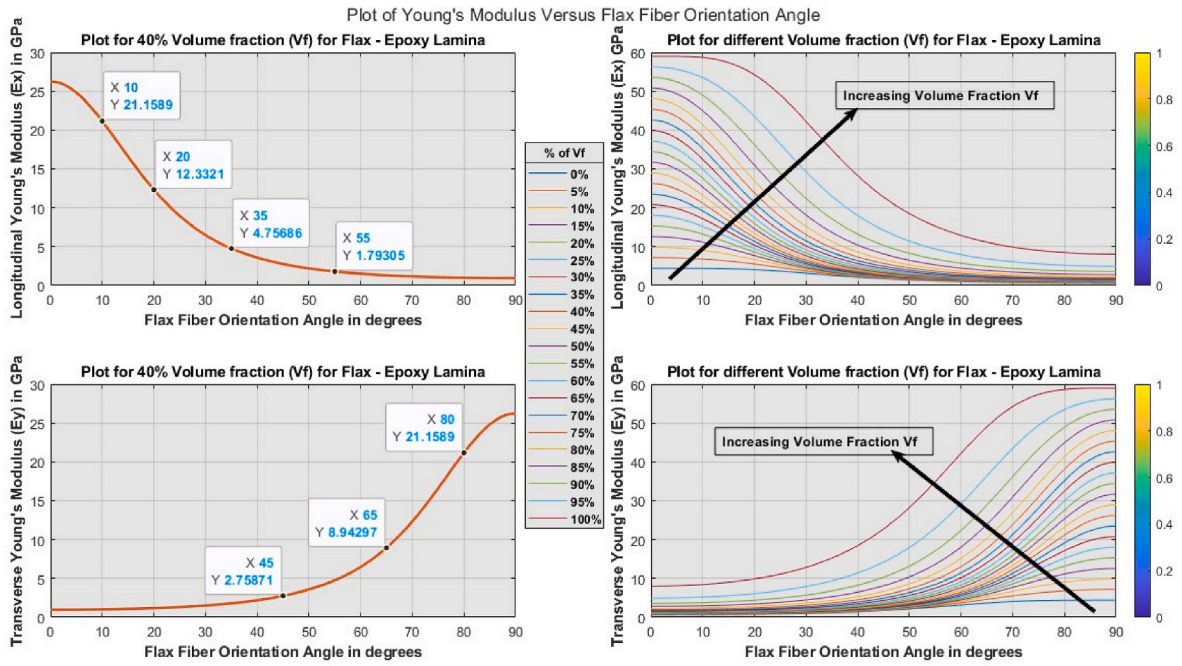

Fig. 5. Changing Young's moduli with fiber orientation for flax-PLA lamina.

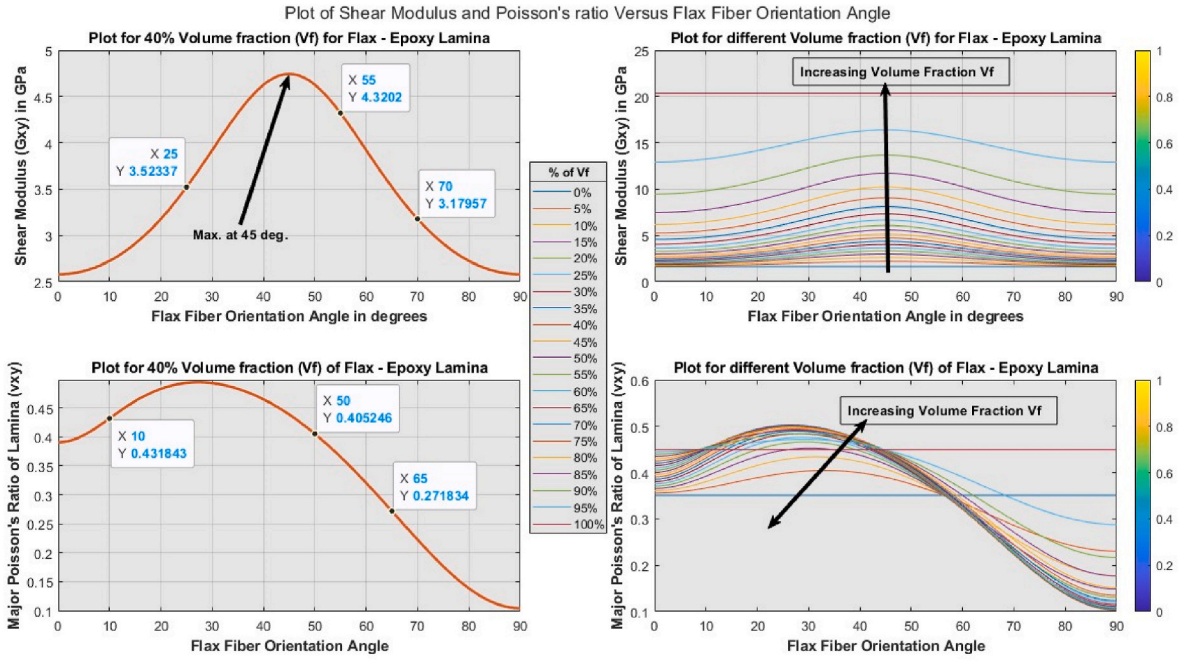

Fig. 6. Changing G_{xy} and ν_{xy} ratio with fiber orientation for flax-PLA lamina.

intriguing since it houses the micro-fibrils. These microfibrils create an angle with the fiber's lengthwise axis, that varies depending on the species, after being encircled the remaining layers [23]. Hemicellulose functions as a contact between cellulose chains and pectin, which is how microfibrils are formed. Essentially, the main wall is composed of pectin and a small number of randomly arranged microfibrils. Because they consist of strands of cellulose that form microfibrils contained within a biological matrix, larger fibrils, and fibers that are at last evident at the microscale, fibers by themselves are therefore regarded as composite materials [24]. A figure illustrating the structural arrangement of natural fibers is provided in Fig. 1. Following sub sections provide a comprehensive overview of bamboo, flax and jute fibers.

2.1. *Bamboo fibers*

These are extracted from bamboo plant, renowned for its quick expansion and environmental friendly characteristics. Cellulose is the primary component, accounting for approximately 60–70 % of the bamboo fiber. Cellulose provides strength and rigidity. Hemicellulose is around 15–25 %, contributing to the flexibility of the bamboo fiber. Lignin is about 10–20 %, giving the bamboo fiber its stiffness and resistance to microbial degradation. Its extractives are small amounts of resins, tannins, and waxes. Diameter of bamboo fibers typically ranges from 10 to 30 μm and density if about 1.2–1.5 g/cm^3. Length of bamboo fiber can vary but generally ranges from 1.5 to 3 mm [26,27]. Bamboo

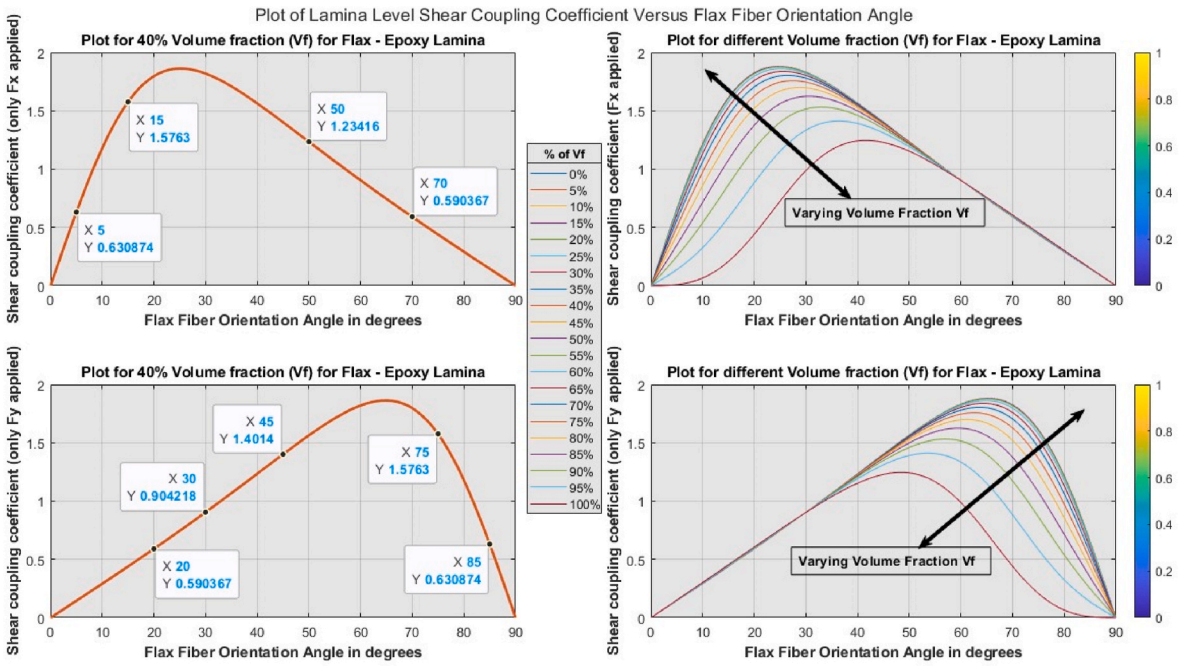

Fig. 7. Changing lamina level shear coupling coefficients with fiber orientation for flax-PLA lamina.

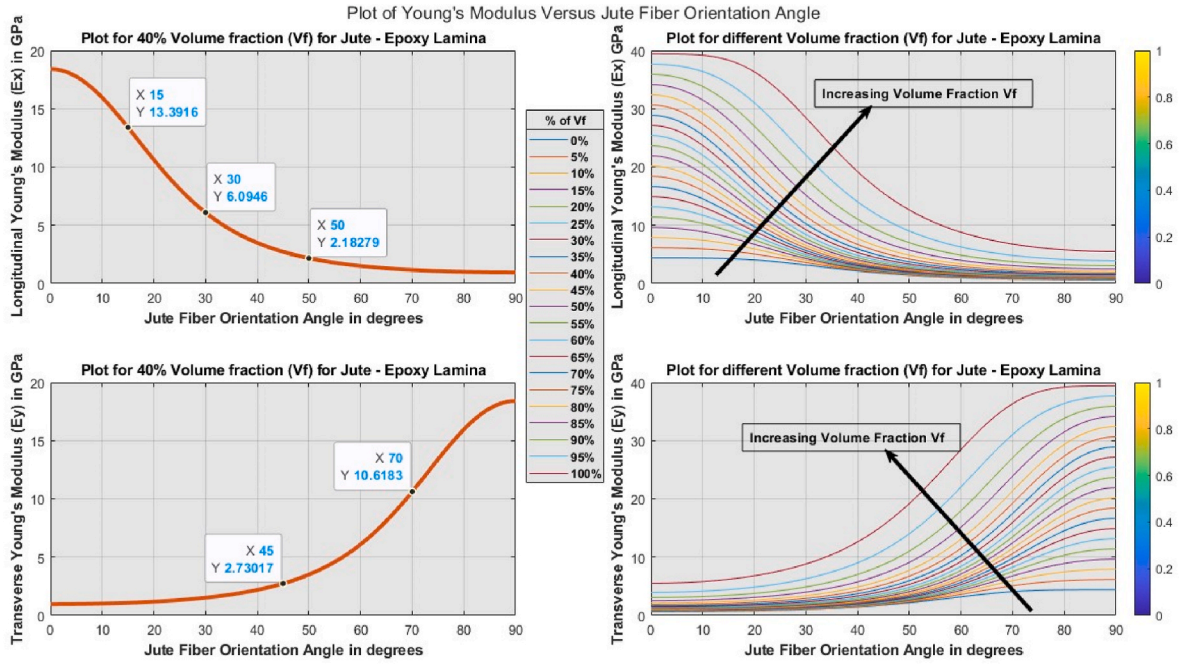

Fig. 8. Changing Young's moduli with fiber orientation for jute-PLA lamina.

has high tensile strength, often around 500–900 MPa, which makes bamboo fibers suitable for reinforcement in composite materials. Its elastic modulus is approximately 30–50 GPa, indicating its stiffness. It has high intake of moisture as a result of cellulose's hydrophilic properties. These fibers have exceptional elongation strength and flexibility, enabling them suitable for a variety of textile and industrial applications. Bamboo fiber elongation at break is typically low, around 1.5–3%, indicating that bamboo fibers do not stretch much before breaking. Bamboo fiber begins to decompose at temperatures above 200 °C (thermal degradation). It has low thermal conductivity, making it a good insulator [27–29]. Mechanical processing involves crushing the bamboo stalks and mechanically separating the fibers. This method retains the fibers' inherent characteristics and structure. Chemical processing involves treating bamboo with chemicals such as sodium hydroxide to obtain fibers. This method produces softer fibers suitable for textiles but may involve environmentally harmful chemicals. Enzymatic processing uses enzymes to break down the non-cellulosic components, offering an eco-friendlier alternative to chemical processing. Composite materials use bamboo as reinforcements in polymers, used in automotive parts, construction materials, and sports equipment. Fast-growing bamboo can be reaped in three to five years, making it a sustainable resource. Bamboo fibers are biodegradable, reducing their environmental footprint when disposed of properly. Bamboo plants absorb significant amounts of CO_2, contributing to carbon sequestration and mitigating

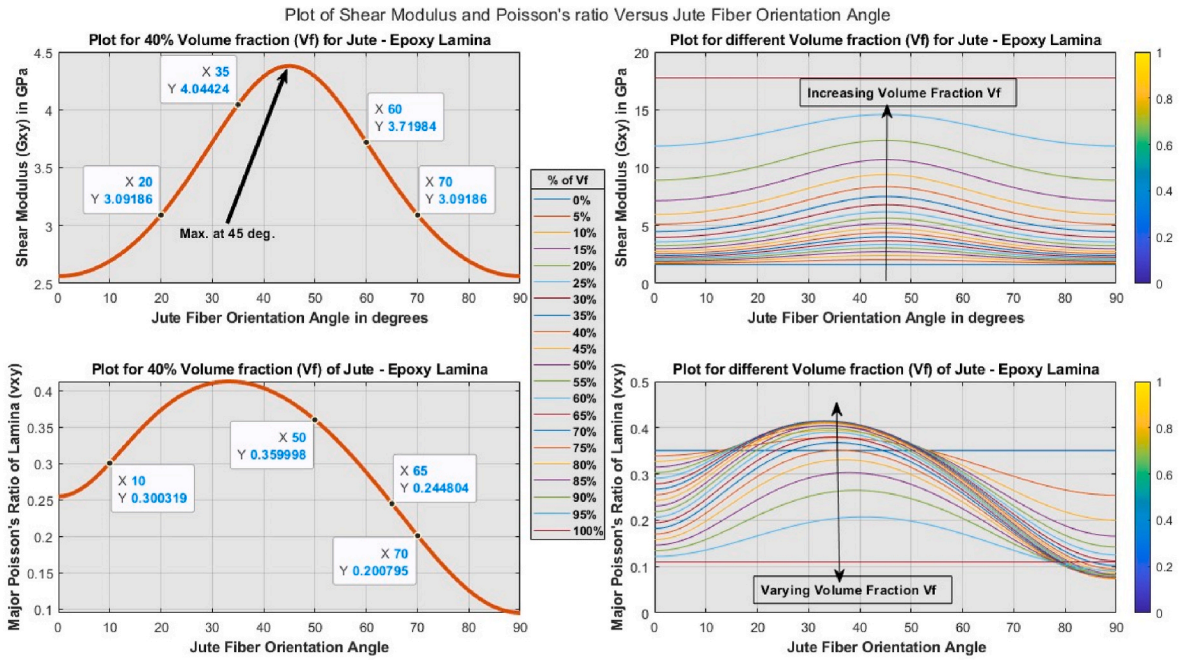

Fig. 9. Changing G_{xy} and ν_{xy} with fiber orientation for jute-PLA lamina.

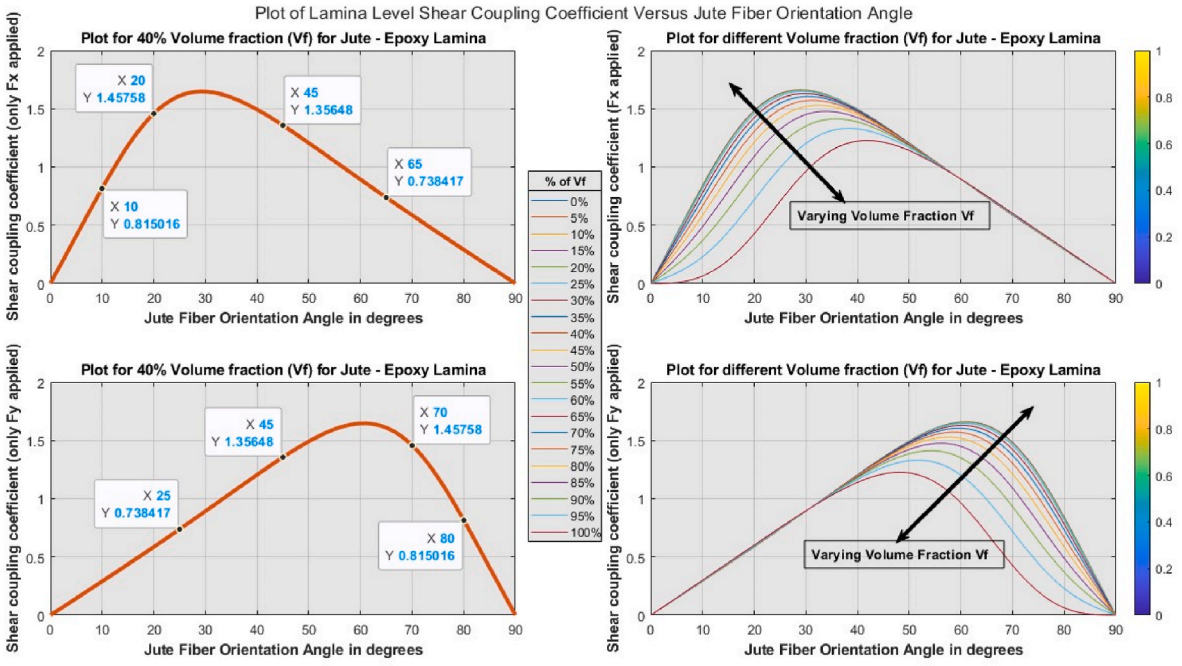

Fig. 10. Changing lamina level shear coupling coefficients with fiber orientation for jute-PLA lamina.

climate change. These properties and characteristics make bamboo fibers an attractive option for a variety of applications, particularly where sustainability and performance are key considerations [26–30].

2.2. Flax fibers

The flax plant (Linum usitatissimum) yields fibers that are prized for robustness, resilience, and eco-friendliness. Flax fibers normally have lengths between 25 and 150 mm, diameter is between 12 and 16 μm, and densities between 1.4 and 1.5 g/cm^3. Flax fiber can range in color from pale blonde to grayish, contingent upon the technique of processing. A flax fiber's tensile strength, Young's modulus, and elongation at break are, respectively, 500–1500 MPa, 60–80 GPa, and 2–3%. Under normal circumstances, thermal degradation begins at 200–220 °C, and 10–12 % of the moisture is recovered. The percentages of cellulose, hemicellulose, lignin, and pectin in flax fibers are 65–75 %, 15–20 %, 2–5% and 2–3%, respectively [31,32]. Flax fibers are fully biodegradable and have lowered carbon footprint compared to synthetic fibers due to less energy-intensive production processes. Flax fibers are utilized in the manufacture of linen fabrics, surgical threads, wound dressings, and premium paper. They are also used in the aerospace and automotive industries as reinforcement in composite materials. The performance and sustainability of flax fibers are being investigated more and more, which makes them a significant resource for a variety of businesses [32].

Table 3
Analogy of Young's moduli E_x and E_y for three lamina.

Fiber Vol. V_f	Fiber Angle	E_x (GPa)			E_y (GPa)		
		BPL	FPL	JPL	BPL	FPL	JPL
20 %	$\theta = 0^0$	21.3256	15.3256	11.4056	0.3026	0.7333	0.7481
	$\theta = 20^0$	7.7104	8.6043	7.5188	0.3810	0.9001	0.9175
	$\theta = 40^0$	1.4436	2.7408	2.7234	0.7947	1.6939	1.7121
	$\theta = 60^0$	0.5132	1.1683	1.1883	3.1262	4.8385	4.6085
	$\theta = 80^0$	0.3203	0.7716	0.7870	16.4806	13.1872	10.3301
	$\theta = 90^0$	0.3026	0.7333	0.7481	21.3256	15.3256	11.4056
40 %	$\theta = 0^0$	38.2442	26.2442	18.4042	0.3955	0.9487	0.9542
	$\theta = 20^0$	10.8262	12.3321	10.6183	0.4977	1.1636	1.1691
	$\theta = 40^0$	1.8924	3.5738	3.5017	1.0384	2.1918	2.1828
	$\theta = 60^0$	0.6703	1.5097	1.5130	4.1563	6.4769	6.0946
	$\theta = 80^0$	0.4186	0.9980	1.0036	26.6836	21.1589	15.9568
	$\theta = 90^0$	0.3955	0.9487	0.9542	38.2442	26.2442	18.4042
60 %	$\theta = 0^0$	55.1628	37.1628	25.4028	0.5704	1.3434	1.3170
	$\theta = 20^0$	15.6155	17.4627	14.6562	0.7178	1.6478	1.6136
	$\theta = 40^0$	2.7296	5.0607	4.8333	1.4978	3.1037	3.0128
	$\theta = 60^0$	0.9668	2.1378	2.0884	5.9949	9.1716	8.4122
	$\theta = 80^0$	0.6037	1.4133	1.3852	38.4879	29.9618	22.0248
	$\theta = 90^0$	0.5704	1.3434	1.3170	55.1628	37.1628	25.4028
80 %	$\theta = 0^0$	72.0814	48.0814	32.4014	1.0229	2.3005	2.1251
	$\theta = 20^0$	26.0615	26.9944	21.3596	1.2876	2.8240	2.6066
	$\theta = 40^0$	4.8795	8.5986	7.7368	2.6861	5.3143	4.8637
	$\theta = 60^0$	1.7346	3.6654	3.3758	10.5668	15.1799	13.0919
	$\theta = 80^0$	1.0828	2.4207	2.2359	55.7052	41.3725	29.3460
	$\theta = 90^0$	1.0229	2.3005	2.1251	72.0814	48.0814	32.4014

Table 4
Comparison of G_{xy} and ν_{xy} for three lamina.

Fiber Vol. V_f	Fiber Angle	G_{xy} (GPa)			ν_{xy}		
		BPL	FPL	JPL	BPL	FPL	JPL
20 %	$\theta = 0^0$	2.0141	1.9987	1.9930	0.3476	0.3708	0.3028
	$\theta = 20^0$	2.4992	2.3983	2.3271	0.4643	0.4500	0.3800
	$\theta = 40^0$	3.7984	3.3494	3.0546	0.4553	0.4469	0.4029
	$\theta = 60^0$	3.1097	2.8653	2.6956	0.3106	0.3217	0.3045
	$\theta = 80^0$	2.1313	2.0977	2.0774	0.1240	0.1608	0.1677
	$\theta = 90^0$	2.0141	1.9987	1.9930	0.0887	0.1308	0.1423
40 %	$\theta = 0^0$	2.6325	2.5804	2.5614	0.3442	0.3906	0.2546
	$\theta = 20^0$	3.3416	3.1796	3.0919	0.4883	0.4829	0.3736
	$\theta = 40^0$	5.4116	4.7439	4.3802	0.4662	0.4646	0.4037
	$\theta = 60^0$	4.2816	3.9219	3.7198	0.3067	0.3204	0.2878
	$\theta = 80^0$	2.8008	2.7259	2.6922	0.1029	0.1384	0.1253
	$\theta = 90^0$	2.6325	2.5804	2.5614	0.0640	0.1041	0.0946
60 %	$\theta = 0^0$	3.7989	3.6398	3.5835	0.3408	0.4104	0.2064
	$\theta = 20^0$	4.8227	4.4809	4.3379	0.4869	0.4939	0.3416
	$\theta = 40^0$	7.8131	6.6698	6.1878	0.4655	0.4707	0.3838
	$\theta = 60^0$	6.1804	5.5209	5.2364	0.3061	0.3255	0.2707
	$\theta = 80^0$	4.0418	3.8441	3.7691	0.1023	0.1436	0.1076
	$\theta = 90^0$	3.7989	3.6398	3.5835	0.0634	0.1094	0.0767
80 %	$\theta = 0^0$	6.8210	6.1749	5.9631	0.3374	0.4302	0.1582
	$\theta = 20^0$	8.4677	7.3870	7.0256	0.4588	0.4887	0.2719
	$\theta = 40^0$	12.8856	10.2423	9.4060	0.4523	0.4706	0.3287
	$\theta = 60^0$	10.5423	8.7941	8.2196	0.3081	0.3418	0.2393
	$\theta = 80^0$	7.2185	6.4758	6.2298	0.1214	0.1815	0.1005
	$\theta = 90^0$	6.8210	6.1749	5.9631	0.0861	0.1518	0.0743

2.3. Jute fibers

Long, silky, and lustrous, jute is a vegetable fiber that may be spun into robust, coarse threads. It is mostly made up of the plant components lignin and cellulose. It contains 60–72 % cellulose, 13–20 % hemicellulose, 12–15 % lignin, 0.2–2% pectin and ash, and 0.4–0.8 % wax. The dimensions of jute fiber are as follows: elongation at break = 1.5–1.8 %, diameter = 20–25 μm, density = 1.48 g/cm^3, tenacity = 2.5–5.0 g/denier (measured in dry condition), and moisture regain = 12–13 %. Typically, jute fiber is lengthened between 1.5 and 4 m. Young's modulus is between 10 and 30 GPa and elongation strength varies from 400 to 800 MPa. Jute decomposes at a temperature of 150–200 °C, and while its flammability is low, its glass transition temperature is poorly defined due to natural fluctuation. However, jute fibers burn easily [33, 34]. Jute fibers break down entirely in soil in six to twelve months because they are biodegradable. Fertilizer and pesticide use in jute farming is quite low. Hessian or burlap cloth, sacks, carpet backing, and curtains are all made from jute fibers. Jute is utilized as reinforcing in composite materials for the building and automotive industries. The processing of jute involves retting, scotching, carding and spinning. Retting is the process of extracting fibers from the jute plant through bacterial action, typically done in water, scotching separates the fibers from the non-fibrous material, carding aligns the fibers and forms them into a continuous web or sliver and spinning converts the sliver into yarn. Jute fibers are prized for their strength, durability, and low cost, rendering them a well-liked option in various industries, particularly for

Table 5
Comparison of lamina level shear coupling coefficients $\eta_{xy,x}$ and $\eta_{xy,y}$ for three lamina.

Fiber Vol. V_f	Fiber Angle	$\eta_{xy,x}$			$\eta_{xy,y}$		
		BPL	FPL	JPL	BPL	FPL	JPL
20 %	$\theta = 0^0$	2.5911	1.5210	1.2121	0.6696	0.5922	0.5888
	$\theta = 20^0$	1.9591	1.5235	1.4479	1.4708	1.2246	1.1959
	$\theta = 40^0$	1.0447	0.9041	0.8938	2.4553	1.6970	1.5190
	$\theta = 60^0$	0.3271	0.2925	0.2915	1.5338	0.8578	0.5868
	$\theta = 80^0$	2.8623	1.7969	1.4576	0.6690	0.5904	0.5862
	$\theta = 90^0$	1.9771	1.5635	1.4919	1.4743	1.2342	1.2061
40 %	$\theta = 0^0$	1.0446	0.9042	0.8933	2.5305	1.8195	1.6465
	$\theta = 20^0$	0.3266	0.2912	0.2898	2.0161	1.1790	0.8150
	$\theta = 40^0$	2.8623	1.7969	1.4576	0.6690	0.5904	0.5862
	$\theta = 60^0$	1.9771	1.5635	1.4919	1.4743	1.2342	1.2061
	$\theta = 80^0$	1.0446	0.9042	0.8933	2.5305	1.8195	1.6465
	$\theta = 90^0$	0.3266	0.2912	0.2898	2.0161	1.1790	0.8150
60 %	$\theta = 0^0$	2.5911	1.5210	1.2121	0.6696	0.5922	0.5888
	$\theta = 20^0$	1.9591	1.5235	1.4479	1.4708	1.2246	1.1959
	$\theta = 40^0$	1.0447	0.9041	0.8938	2.4553	1.6970	1.5190
	$\theta = 60^0$	0.3271	0.2925	0.2915	1.5338	0.8578	0.5868
	$\theta = 80^0$	2.5911	1.5210	1.2121	0.6696	0.5922	0.5888
	$\theta = 90^0$	1.9591	1.5235	1.4479	1.4708	1.2246	1.1959
80 %	$\theta = 0^0$	1.0447	0.9041	0.8938	2.4553	1.6970	1.5190
	$\theta = 20^0$	0.3271	0.2925	0.2915	1.5338	0.8578	0.5868
	$\theta = 40^0$	2.8623	1.7969	1.4576	0.6690	0.5904	0.5862
	$\theta = 60^0$	1.9771	1.5635	1.4919	1.4743	1.2342	1.2061
	$\theta = 80^0$	1.0446	0.9042	0.8933	2.5305	1.8195	1.6465
	$\theta = 90^0$	0.3266	0.2912	0.2898	2.0161	1.1790	0.8150

environmentally friendly products [35].

3. Macromechanics of lamina based analytical study

Lamina is a basic form of continuous fiber reinforced composites where a large number of fibers are impregnated into matrix whereas laminate is a stack of laminas. Lamina is thin and thickness of lamina is very small compared to other dimensions. Lamina is heterogeneous and anisotropic. Heterogeneous means stress strain relation at point on the matrix is different than at a point on the fiber [36]. Anisotropic means the properties with respect to an axis are dependent on the orientation of the axis. However, a unidirectional lamina is orthotropic, because of 3 mutually perpendicular planes of material property symmetry (Principal material axis 1-2-3). Therefore, unidirectional lamina is not fully anisotropic, it requires 9 elastic constants. It can be noted here that unidirectional lamina should be considered as transversely isotropic only when they are arranged in a square array, in that case it requires 5 elastic constants. In specially orthotropic lamina, analysis axes (x-y-z) coincides with the material axes (1-2-3). In generally orthotropic lamina analysis axes (x-y-z) doesn't coincide with the material axes (1-2-3) [37, 38]. Actually lamina is heterogeneous, the properties are location dependent, because it consists of fiber and matrix. But in macromechanics of lamina, lamina is assumed homogeneous – represented by the average properties. Other assumptions include, Hooke's law is applicable, small deformation theory is followed and plane stress situation exists i.e. no out of plane stress [36].

A typical lamina is very thin compared to its inplane dimensions and in absence of out-of-plane load, it is assumed to be in plane state of stress. If there are no out of plane loads in direction three, then it is a case of plane stress. Therefore, in 2D lamina, only three components of stresses are present. The conditions of plane stress include, $\sigma_1 \neq 0$, $\sigma_2 \neq 0$, $\tau_{12} \neq 0$, $\sigma_3 = 0$, $\tau_{23} = 0$ and $\tau_{13} = 0$ but $\varepsilon_1 \neq 0, \varepsilon_2 \neq 0$, $\varepsilon_3 \neq 0$, $\gamma_{12} \neq 0$, $\gamma_{23} = 0$ and $\gamma_{13} = 0$. If we substitute these inplane stress conditions in the stress strain relations, we get the equation for strains and stresses for a lamina. The engineering constants of lamina in the loading axes or global axes or analysis axes i.e. E_x, E_y, ν_{xy}, G_{xy}, $\eta_{xy,x}$, $\eta_{xy,y}$ are related to the engineering constants in the material axes i.e. E_1, E_2, ν_{12}, G_{12} by equations (i)–(vi) [39].

$$\frac{1}{E_x} = \frac{1}{E_1}c^4 + \left(\frac{1}{G_{12}} - \frac{2\nu_{12}}{E_1}\right)c^2s^2 + \frac{1}{E_2}s^4 \quad \text{(i)}$$

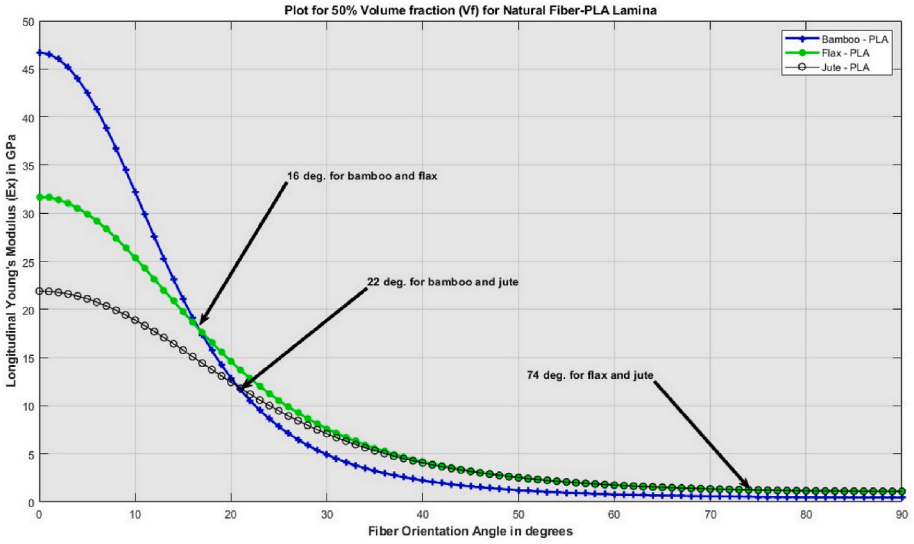

Fig. 11. Comparison of changes in the behavior of E_x for three lamina.

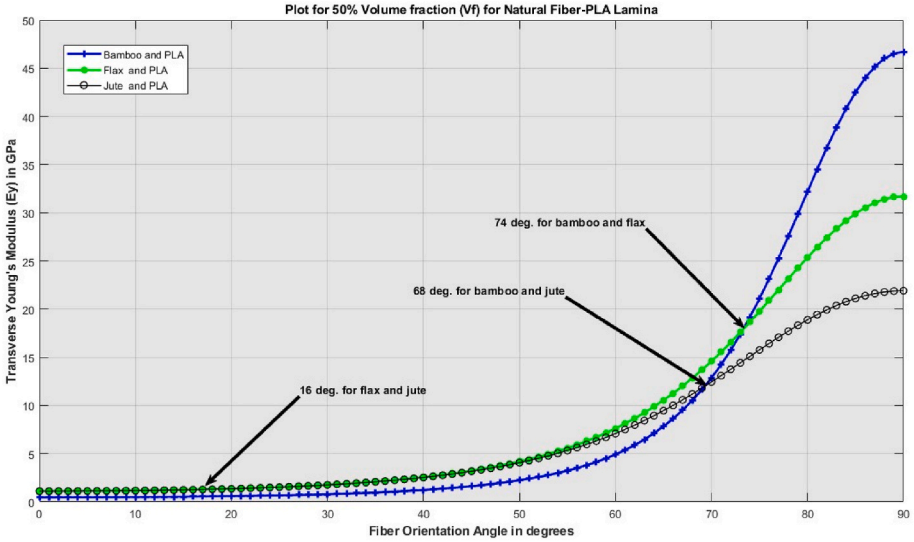

Fig. 12. Comparison of changes in the behavior of E_y for three lamina.

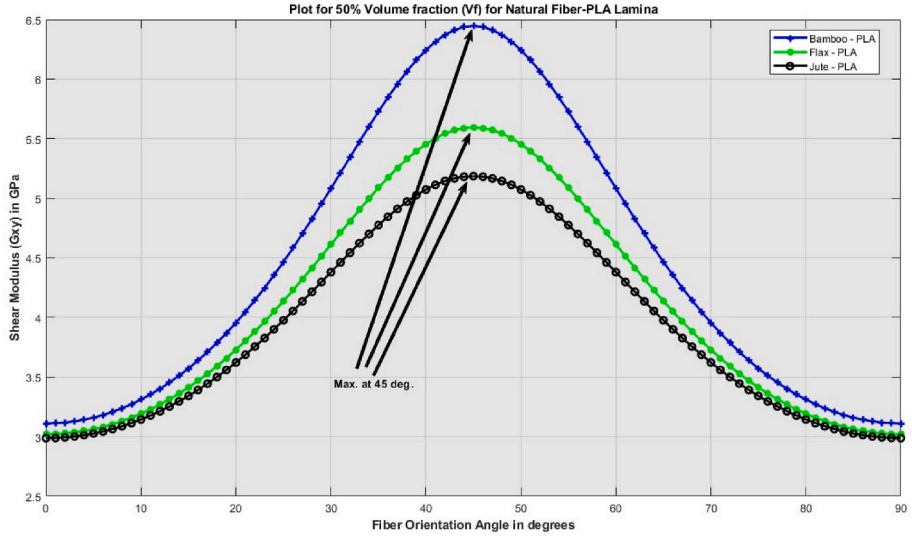

Fig. 13. Comparison of changes in shear modulus G_{xy} for three lamina.

$$\frac{1}{E_y}=\frac{1}{E_1}s^4+\left(\frac{1}{G_{12}}-\frac{2\nu_{12}}{E_1}\right)s^2c^2+\frac{1}{E_2}c^4 \tag{ii}$$

$$\nu_{xy}=E_x\left[\frac{\nu_{12}}{E_1}\left(s^4+c^4\right)-\left(\frac{1}{E_1}+\frac{1}{E_2}-\frac{1}{G_{12}}\right)s^2c^2\right] \tag{iii}$$

$$G_{xy}=2\left(\frac{2}{E_1}+\frac{2}{E_2}+\frac{4\nu_{12}}{E_1}-\frac{1}{G_{12}}\right)c^2s^2+\frac{1}{G_{12}}\left(s^4+c^4\right) \tag{iv}$$

$$\eta_{xy,x}=E_x\left[\left(\frac{2}{E_1}+\frac{2\nu_{12}}{E_1}-\frac{1}{G_{12}}\right)sc^3-\left(\frac{2}{E_2}+\frac{2\nu_{12}}{E_1}-\frac{1}{G_{12}}\right)s^3c\right] \tag{v}$$

$$\eta_{xy,y}=E_y\left[\left(\frac{2}{E_1}+\frac{2\nu_{12}}{E_1}-\frac{1}{G_{12}}\right)s^3c-\left(\frac{2}{E_2}+\frac{2\nu_{12}}{E_1}-\frac{1}{G_{12}}\right)sc^3\right] \tag{vi}$$

where, E_x and E_y are the longitudinal and transverse Young's moduli of lamina respectively in the analysis axes, ν_{xy} is the major Poisson's ratio in the analysis axes, G_{xy} is the shear modulus in the analysis axes, $\eta_{xy,x}$ and $\eta_{xy,y}$ are the lamina level shear coupling coefficient when only F_x and F_y is applied respectively in the analysis axes, E_1 and E_2 are the longitudinal and transverse Young's moduli respectively in the material axes, ν_{12} is the major Poisson's ratio in the material axes, G_{12} is the shear modulus in material axes and c and s are cosine and sine of fiber orientation angle θ [39].

The engineering constants in the material axes are obtained using the micromechanics of lamina approach. The key assumptions in the micromechanics of lamina include, perfect bonding between fiber and matrix, elastic moduli, diameter and distance between fibers is uniform, fibers are homogeneous, continuous and parallel, fibers and matrix are isotropic and follow Hooke's law, fibers possess consistent strength and lamina is free from voids [39]. The E_1 and E_2 in material axes are obtained from equations (vii) and (viii). The ν_{12} and G_{12} in material axes are obtained from equations (ix) to (x) respectively.

$$E_1=E_fV_f+E_mV_m \tag{vii}$$

$$\frac{1}{E_2}=\frac{V_f}{E_f}+\frac{V_m}{E_m} \tag{viii}$$

$$\nu_{12}=\nu_fV_f+\nu_mV_m \tag{ix}$$

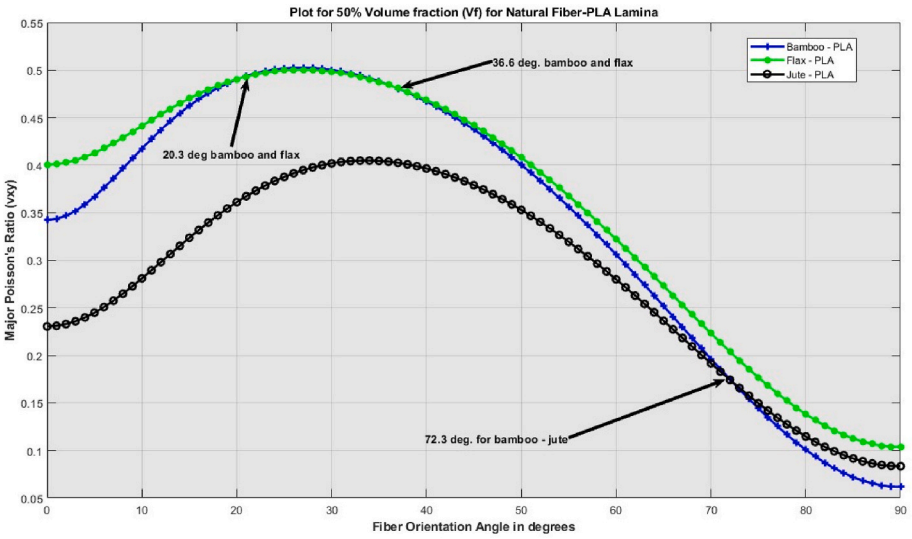

Fig. 14. Comparison of changes in Poisson's ratio ν_{xy} for three lamina.

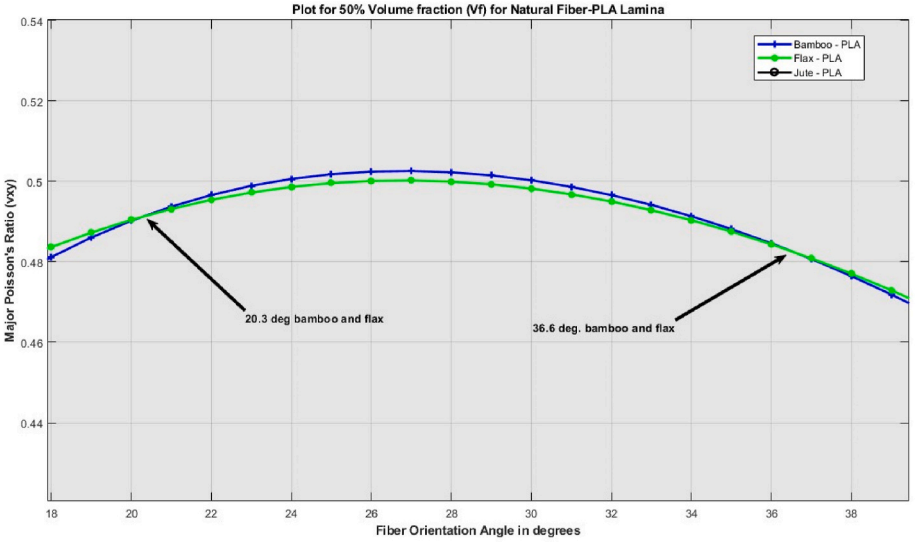

Fig. 15. Focused view of variation of Poisson's ratio ν_{xy} between bamboo and flax – PLA lamina.

$$\frac{1}{G_{12}} = \frac{V_f}{G_f} + \frac{V_m}{G_m} \tag{x}$$

where, E_f and E_m are the Young's moduli of fiber and matrix respectively, ν_f and ν_m are the major Poisson's ratio of fiber and matrix respectively, G_f and G_m are the shear moduli of fiber and matrix respectively and V_f and V_m are the volume fraction of fiber and matrix respectively ($V_f + V_m = 1$). The shear modulus can be obtained from relation $G = E/[2(1+\nu)]$ [39,40]. The fiber and matrix engineering constant values are compiled from numerous research publications that include experimental findings. A range for the Yong's moduli in longitudinal and transverse direction based on the experimental results have all been provided in various publications for natural fiber [24,36–40]. The range of engineering constant values for the PLA matrix and three natural fibers, respectively, employed for the analytical analysis in this article are provided in Tables 1 and 2.

The engineering constants of lamina, namely stiffness, strength, and thermal expansion, are heavily reliant upon the orientation of the fibers, represented by the symbol θ. The E_x, E_y, G_{12}, ν_{12}, $\eta_{xy,x}$, $\eta_{xy,y}$ and thermal expansion coefficients α_x and α_y are the primary engineering constants in composites that are impacted by fiber orientation. This paper examines all engineering constants, excluding the thermal expansion coefficient. It should be noted here that there is difference between engineering constants and elastic constants, engineering constants are experimentally measurable quantities and elastic constants are theoretical quantities and can't be measured experimentally. But elastic constants can be expressed in terms of engineering constants which are given by mathematical equations. When fibers are oriented in a parallel manner toward the load direction (0° orientation), the composite has a high longitudinal modulus (E_x) that approaches the modulus of the individual fiber. The fibers bear the majority of the load, which explains this. When fibers are aligned perpendicular (90^0) to the load direction, or when the fibers have a lower transverse modulus (E_y), it is because the load is supported by the matrix material, which generally has a lower modulus than the fibers [39]. The off-axis modulus changes for fiber orientations that range from 0° to 90°. Both the matrix's and the fibers' contributions to stiffness can be taken into account when computing it using macro- and micromechanics models. Fiber direction affects the in-plane shear modulus (G_{xy}). Fibers make a substantial contribution to the shear stiffness for 0° orientations. Because of the interaction between

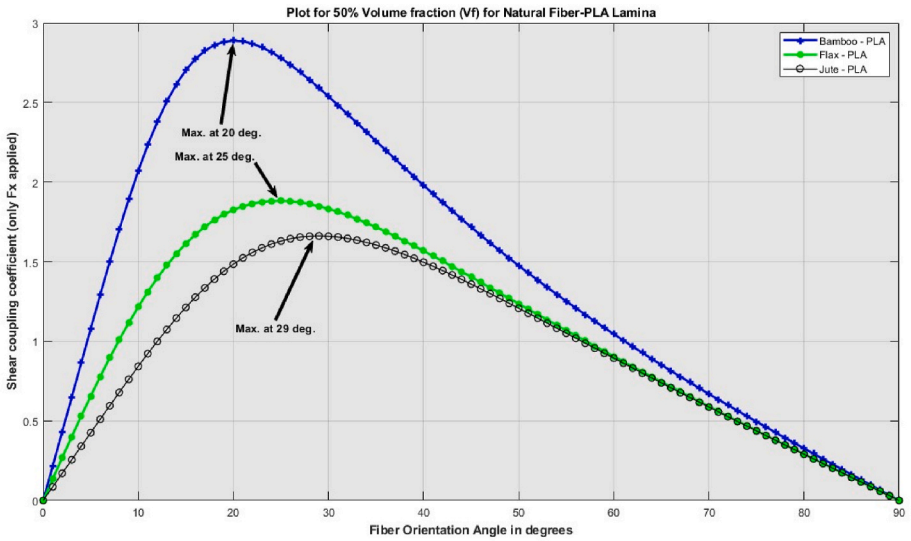

Fig. 16. Comparison of variations of lamina level shear coupling coefficient $\eta_{xy,x}$ for three lamina.

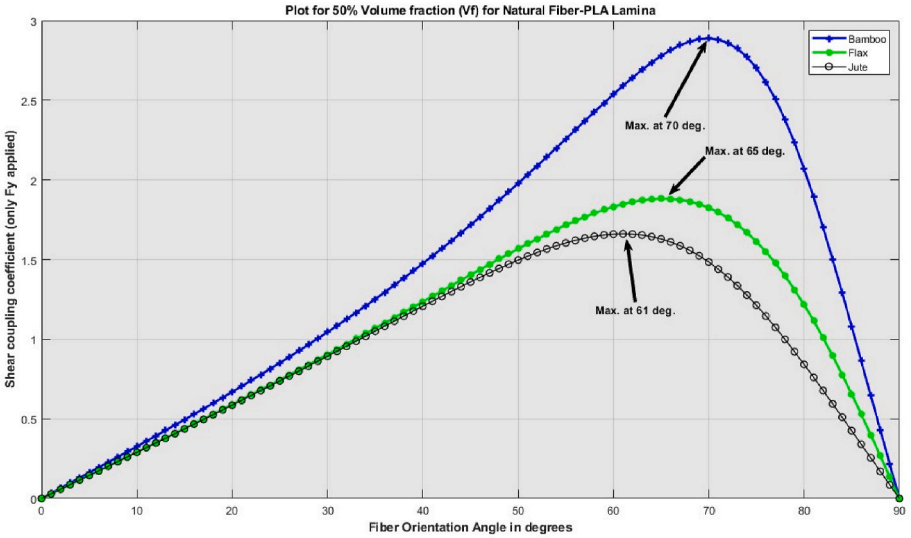

Fig. 17. Comparison of variations of lamina level shear coupling coefficient $\eta_{xy,y}$ for three lamina.

the fibers and matrix, shear characteristics for 45° orientations are ideal, resulting in a balanced transfer of stress. Off-axis shear modulus is comparable to elastic modulus; macromechanics and micromechanics models that account for the stiffness contributions from the matrix and fibers can be used to estimate the shear modulus at other angles. The fiber orientation and the manner in which the fibers and matrix engage determine ν_{xy}. ν_{yx} is mostly determined by the fiber properties for 0° orientations; for other orientations, it is dependent on both fiber and matrix properties. Minor Poisson's ratio (ν_{yx}) is more influenced by the fiber-matrix contact and matrix characteristics [39].

In practical applications, the choice of fiber orientation is dictated by the desired balance of mechanical properties. For example, cross-ply layup (0°/90° orientation) provides balanced properties in two perpendicular directions, quasi-isotropic layup (multiple angles) mimics isotropic materials and provides uniform properties in all directions, and unidirectional layup (0° orientation) is used for components requiring high stiffness and strength in one direction. Composite material engineering constants are strongly influenced by fiber orientation. Engineers can modify the mechanical properties of composites to satisfy particular application needs by meticulously choosing the orientation of the fibers [39]. The best laminate design uses analytical techniques, numerical simulations, and experimental methods to anticipate and validate these features. We have applied analytical approaches in this paper. The next part contains the findings of the analytical investigation for various fiber orientation angles.

4. Results of analytical study on the natural fiber PLA lamina

Bamboo-PLA lamina, flax-PLA lamina and jute PLA lamina are the three laminas in this sequence for which the results are shown in this section. Six engineering constants of natural fiber PLA lamina are shown to vary with fiber orientation θ from 0^0 to 90^0 (in steps of 1^0) for various fiber volume fractions (in steps of 5 %). The E_x, E_y, G_{xy}, ν_{xy}, $\eta_{xy,x}$ and $\eta_{xy,y}$ are the six engineering constants.

Fig. 2 illustrates how the E_x and E_y of the bamboo-PLA lamina vary when the fiber orientation angle increases for both the 40 % fiber volume fraction and the entire fiber volume fraction that increases from 0 % (fully matrix) to 100 % (fully fibers). It can be observed that E_x is maximum at 0^0 bamboo fiber alignment and reaches to minimum value at 90^0 bamboo fiber alignment for all the values of V_f. In case of E_y, it is

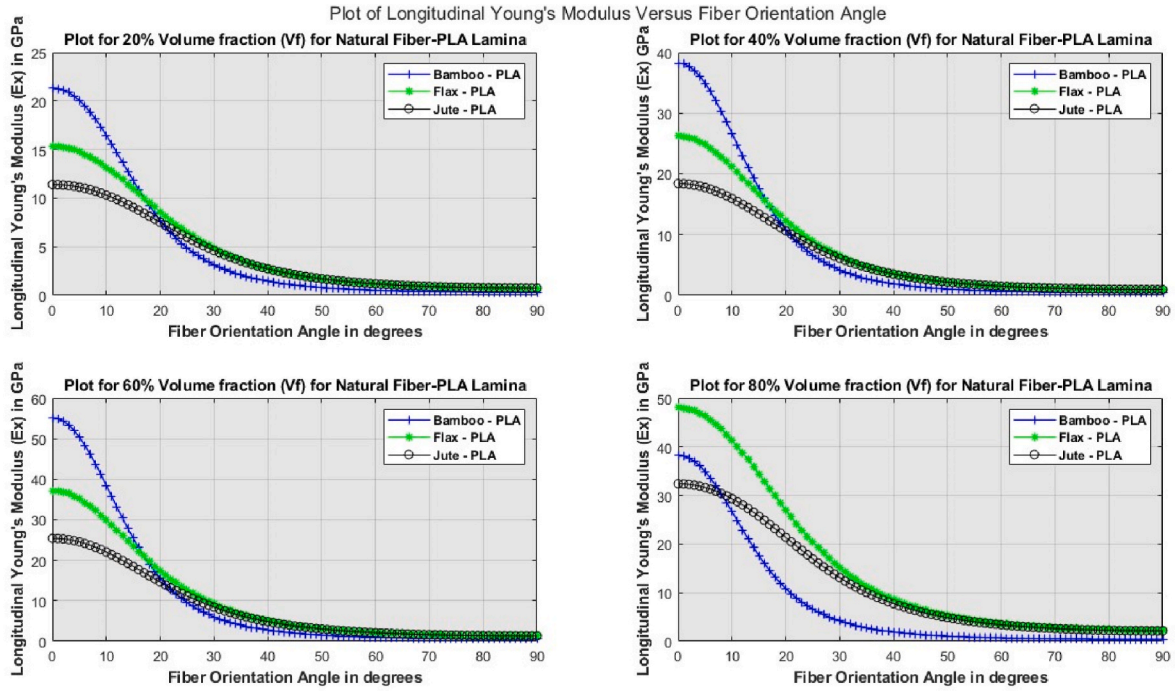

Fig. 18. Changes in the behavior of E_x due to varied volume fraction V_f.

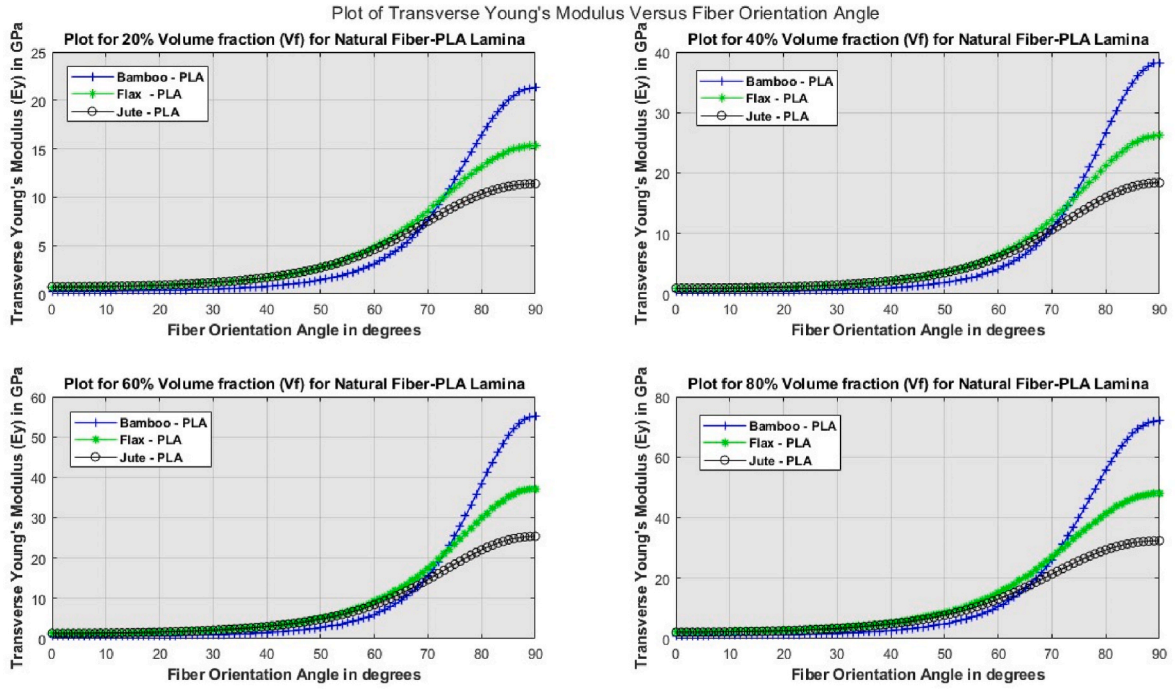

Fig. 19. Changes in the behavior of E_y due to varied volume fraction V_f.

minimum value at 0^0 bamboo fiber alignment and reaches maximum at 90^0 bamboo fiber alignment for all the values of V_f. Similar to this, Fig. 3 illustrates how the G_{xy} and ν_{xy} of bamboo-PLA lamina vary as the fiber alignment angle rises. It can be seen that G_{xy} reaches maximum at 45^0 bamboo fiber alignment and is zero at 0^0 and 90^0 bamboo fiber alignment. In case of ν_{xy}, it rises and reaches maximum at certain bamboo fiber alignment and reduces up to bamboo fiber alignment of approximately 55^0. Also for a given V_f the value of ν_{xy} is maximum below 55^0 and beyond 55^0 it is minimum at all bamboo fiber orientation angle. Fig. 4 also illustrates how the lamina level shear coupling coefficients $\eta_{xy,x}$ and $\eta_{xy,y}$ (when F_x and F_y are applied separately) of bamboo-PLA lamina vary as the fiber alignment angle rises from 0^0 to 90^0. Very interesting observation can be made seen here up to the fiber alignment of approximately 50^0. The values of $\eta_{xy,x}$ decreases as V_f is increased at a given bamboo fiber alignment up to 50^0 but beyond that $\eta_{xy,x}$ have almost same value for all the values of V_f at a given bamboo fiber alignment. $\eta_{xy,y}$ have almost same value for all the values of V_f at a given bamboo fiber alignment up to approximately 40^0 bamboo fiber alignment but beyond that angle of fiber alignment $\eta_{xy,y}$ decreases as V_f is increased at a given bamboo fiber alignment.

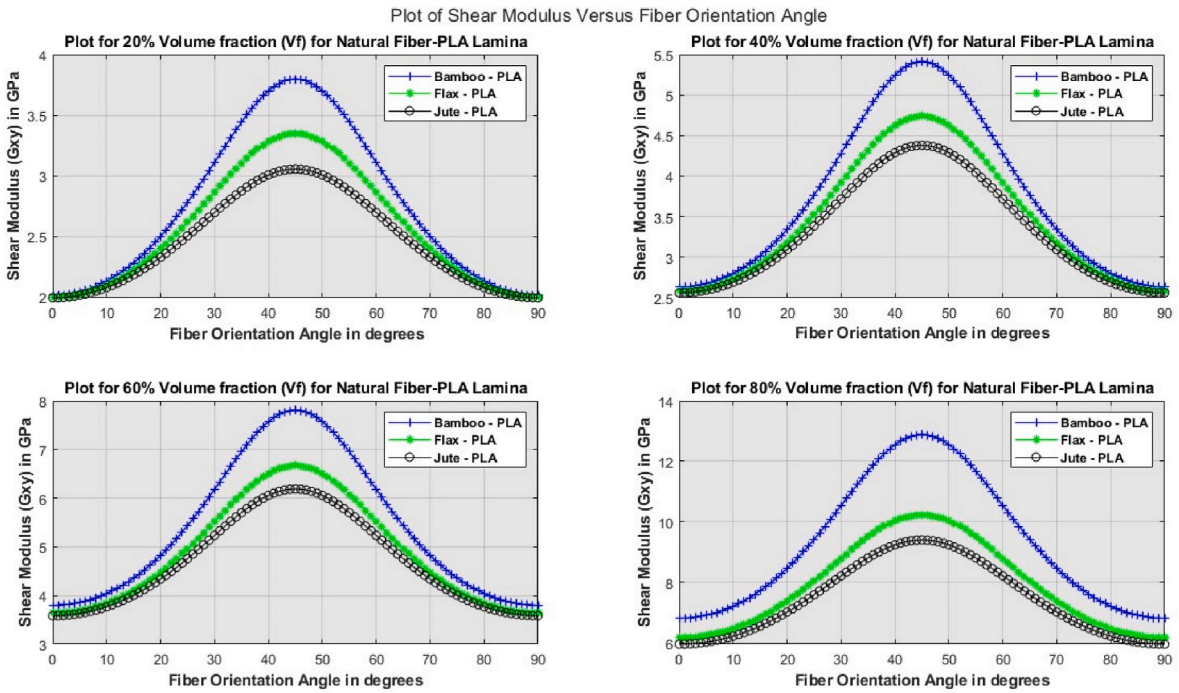

Fig. 20. Changes in the behavior of G_{xy} due to varied volume fraction V_f.

Table 6
Angles at which maximum ν_{xy}, $\eta_{xy,x}$ and $\eta_{xy,y}$ are obtained.

V_f (%)	Poisson's ratio			Lamina shear coupling coefficients					
	ν_{xy}			$\eta_{xy,x}$			$\eta_{xy,y}$		
	BPL	FPL	JPL	BPL	FPL	JPL	BPL	FPL	JPL
5	32^0	33^0	35^0	29^0	36^0	38^0	61	54^0	52^0
10	31^0	31^0	34^0	26^0	33^0	36^0	64^0	57^0	54^0
15	29^0	30^0	34^0	24^0	31^0	34^0	66^0	59^0	56^0
20	29^0	29^0	33^0	16^0	29^0	32^0	67^0	61^0	58^0
25	28^0	29^0	33^0	22^0	27^0	31^0	68^0	63^0	59^0
30	27^0	28^0	33^0	21^0	26^0	30^0	69^0	64^0	60^0
35	27^0	28^0	33^0	21^0	26^0	30^0	69^0	64^0	60^0
40	27^0	27^0	33^0	20^0	25^0	29^0	70^0	65^0	61^0
45	27^0	27^0	33^0	20^0	25^0	29^0	70^0	65^0	61^0
50	27^0	27^0	34^0	20^0	25^0	29^0	70^0	65^0	61^0
55	27^0	27^0	34^0	20^0	25^0	29^0	70^0	65^0	61^0
60	27^0	27^0	34^0	20^0	25^0	29^0	70^0	65^0	61^0
65	27^0	27^0	35^0	21^0	26^0	30^0	69^0	64^0	60^0
70	28^0	27^0	35^0	21^0	26^0	30^0	69^0	64^0	60^0
75	28^0	27^0	36^0	22^0	27^0	31^0	68^0	63^0	59^0
80	29^0	27^0	37^0	16^0	29^0	32^0	67^0	61^0	58^0
85	30^0	27^0	38^0	24^0	31^0	34^0	66^0	59^0	56^0
90	31^0	28^0	39^0	26^0	33^0	36^0	64^0	57^0	54^0
95	33^0	29^0	41^0	29^0	36^0	38^0	61^0	54^0	52^0

For a 40 % fiber volume fraction as well as for all fiber volume fractions increased from 0 % (totally matrix) to 100 % (absolutely fibers), Fig. 5 illustrates the changing E_x and E_y of flax-PLA lamina with rising fiber alignment ranging from 0^0 to 90^0. For all values of V_f, it can be shown that E_x reaches its smallest value at 90^0 flax fiber alignment and reaches its highest at 0^0 flax fiber alignment. For all values of V_f, the value of E_y is at its lowest at 0^0 flax fiber alignment and at its highest at 90^0 flax fiber alignment. Fig. 6 demonstrates the changes in the G_{xy} and ν_{xy} of flax-PLA lamina with increasing fiber orientation angle. 45^0 flax fiber alignment is where G_{xy} reaches its highest, whereas 0^0 and 90^0 flax fiber alignment are where G_{xy} is zero. When it comes to ν_{xy}, it increases, achieves its peak at a specific flax fiber alignment, and then decreases to a flax fiber alignment of roughly 50^0. For any flax fiber orientation angle, the value of ν_{xy} is minimal at an angle of 50^0 (approximately) and highest below 50^0 for a given V_f. The latter two figures in Fig. 7 also show the changes in the lamina level shear coupling coefficients of the flax-PLA lamina with increasing fiber orientation angle when F_x and F_y are applied separately. When V_f is increased at a certain flax fiber alignment, the values of $\eta_{xy,x}$ fall up to 58^0; beyond that, $\eta_{xy,x}$ virtually always has the same value for all values of V_f at a given flax fiber alignment. Up to around 32^0 flax fiber alignment, $\eta_{xy,y}$ has almost the same value for all values of V_f at a given flax fiber alignment; however, beyond that angle of fiber alignment, $\eta_{xy,y}$ declines as V_f is increased at a given flax fiber alignment.

With an increasing fiber orientation angle, Fig. 8 illustrates the fluctuation in the E_x and E_y of the jute-PLA lamina for both the 40 % fiber content and the entire fiber volume fraction increased from 0 % (completely matrix) to 100 % (entirely fibers). E_x is seen to be at its highest for all values of V_f at 0^0 jute fiber alignment and to be at its lowest at 90^0 jute fiber alignment. For all values of V_f, the smallest value of E_y is at 0^0 jute fiber alignment, and the maximum value is at 90^0 jute fiber alignment. Similarly, Fig. 9 illustrates how G_{xy} and ν_{xy} of jute-PLA lamina change as the fiber alignment angle rises. As can be observed, G_{xy} is zero at 0^0 and 90^0 jute fiber alignment and reaches its maximum at 45^0 jute fiber alignment. Regarding ν_{xy}, it increases to a maximum at a specific jute fiber alignment and then decreases to a jute fiber alignment of about 80^0. Additionally, the value of ν_{xy} for a given V_f reaches its maximum below 80^0 and its minimum beyond 80^0 at all jute fiber orientation angles. Fig. 10 illustrates how the lamina level shear coupling coefficients (assuming F_x and F_y are applied separately) of jute-PLA lamina change as the fiber alignment angle rises from 0^0 to 90^0. Up to 55^0, the values of $\eta_{xy,x}$ drop when V_f is increased at a certain jute fiber alignment; after that, $\eta_{xy,x}$ almost always have the same value for all values of V_f at a particular jute fiber alignment. Up to around 35^0 jute fiber alignments, $\eta_{xy,y}$ has almost the same value for all values of V_f at a given jute fiber alignment; however, as V_f is increased at a given jute fiber alignment beyond that point, $\eta_{xy,y}$ drops.

The following tables compare the variations in engineering constants of bamboo-PLA lamina (BPL), flax-PLA lamina (FPL) and jute-PLA lamina (JPL) for a few chosen volume fractions and fiber orientation angles. The variations of Young's moduli are compared in Table 3, the variations of G_{xy} and ν_{xy} of laminas are compared in Table 4 and the

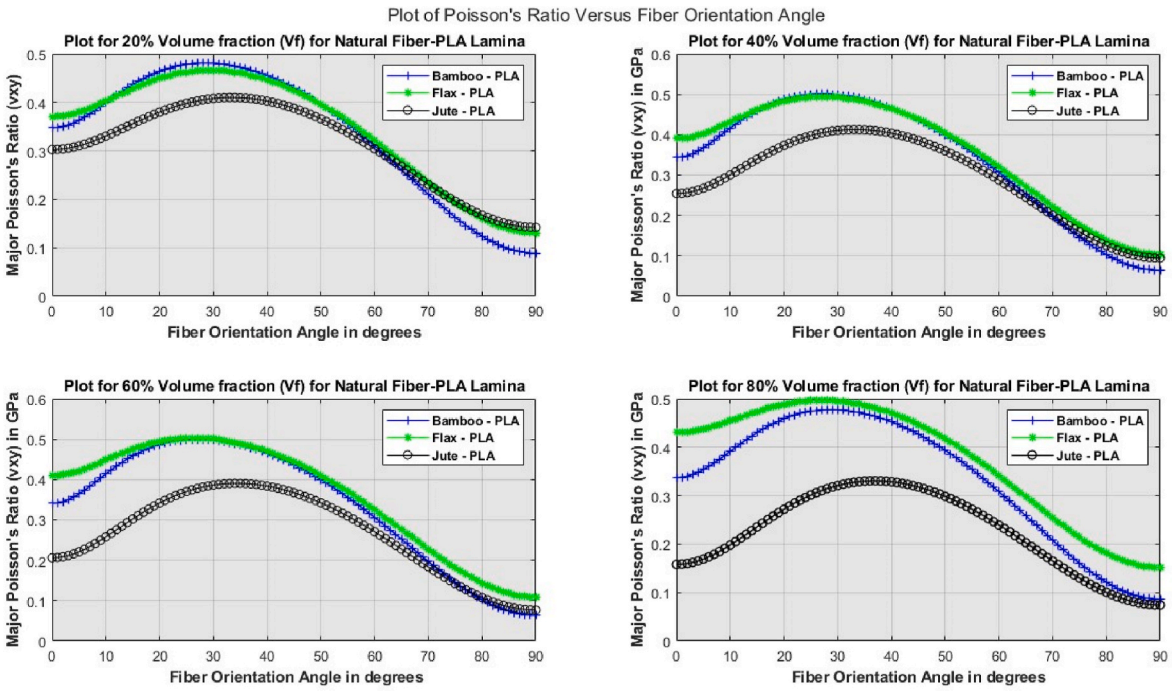

Fig. 21. Changes in the behavior of v_{xy} due to varied volume fraction V_f.

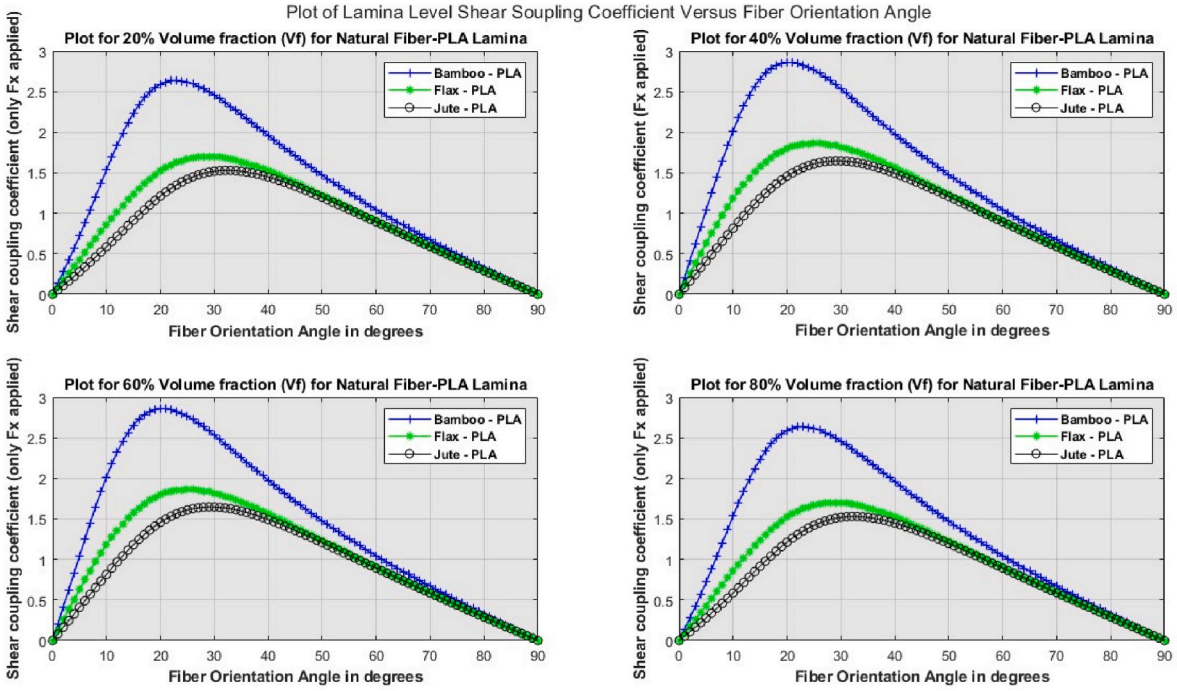

Fig. 22. Changes in the behavior of shear coupling coefficient $\eta_{xy,x}$ due to varied volume fraction V_f.

variations of $\eta_{xy,x}$ and $\eta_{xy,y}$ are compared in Table 5.

The following figures show plots that compare the engineering constants variation for a 50 % fiber volume percentage with the orientation of the fibers. The variations of E_x and E_y are compared in Figs. 11 and 12, respectively, the comparison of the fluctuation in the lamina's G_{xy} and ν_{xy} is shown in Figs. 13 and 14, respectively and Figs. 17 and 18 demonstrate the variation of $\eta_{xy,x}$ and $\eta_{xy,y}$ respectively. From Fig. 11 it can be observed that up to 16^0 fiber alignment E_x of bamboo-PLA lamina is more than that of the flax-PLA lamina and beyond 16^0 E_x of flax-PLA lamina is more than that of bamboo-PLA lamina. And up to 22^0 fiber orientation angle E_x of bamboo-PLA lamina is more than that of jute-PLA lamina and beyond 22^0 fiber alignment E_x of jute-PLA lamina is more than that of bamboo-PLA lamina. Similarly, up to 74^0 fiber orientation angle E_x of flax-PLA lamina is more than that of jute-PLA lamina and beyond 74^0 fiber orientation angle E_x of jute-PLA lamina more than that of flax-PLA and bamboo-PLA laminae. From Fig. 12 it can be observed that up to 74^0 fiber alignment E_y of flax-PLA lamina is more than that of the bamboo-PLA lamina and beyond 74^0 E_y of bamboo-PLA lamina is more than that of flax-PLA and jute-PLA laminae. And up to 68^0 fiber orientation angle E_y of jute-PLA lamina is more than that of bamboo-PLA

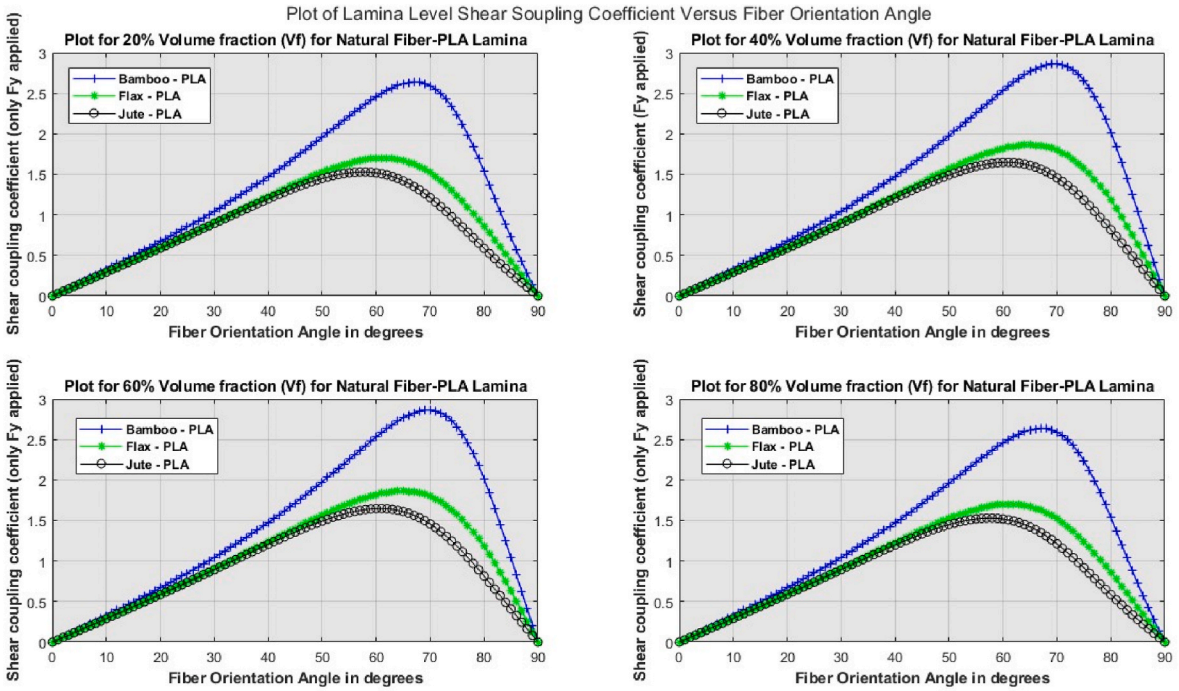

Fig. 23. Changes in the behavior of shear coupling coefficient $\eta_{xy,y}$ due to varied volume fraction V_f.

lamina and beyond 68^0 fiber alignment E_y of bamboo-PLA lamina is more than that of jute-PLA lamina. Similarly, up to 16^0 fiber orientation angle E_y of jute-PLA lamina is more than that of flax-PLA and bamboo-PLA laminae, and beyond 16^0 fiber orientation angle E_y of flax-PLA lamina is more than that of jute-PLA lamina. From Fig. 13 it can be noted that at all fiber all fiber orientation angle bamboo-PLA has maximum G_{xy} followed by flax-PLA lamina and as expected all three PLA based laminae have shown maximum value of G_{xy} at 45^0. From Fig. 14 it can be seen that up to approximately 20^0 fiber alignment ν_{xy} of flax-PLA lamina is more than that of bamboo-PLA and jute-PLA laminae. Beyond fiber orientation of approximately 37^0 flax-PLA lamina is more than other two laminae. Bamboo-PLA lamina not only has maximum ν_{xy} of all three laminae between fiber orientations approximately 20^0 and 37^0 but also has minimum ν_{xy} beyond approximately 72^0 of fiber alignment. Also from Figs. 16 and 17 it can be seen that bamboo-PLA lamina has highest $\eta_{xy,x}$ and $\eta_{xy,y}$ followed by flax-PLA and jute-PLA laminae at all fiber orientations, also the fiber orientations at which $\eta_{xy,x}$ and $\eta_{xy,y}$ reach maximum are depicted.

5. Discussion and conclusion

Numerous helpful details, some of which are covered below, can be gleaned from the data of variations of engineering constants with the fiber orientation angle for different volume fractions for bamboo-PLA lamina, flax-PLA lamina and jute-PLA lamina. From Figs. 2, 5 and 8 it is evident that for all the given volume fractions, E_x of lamina is maximum at 0^0 and minimum at 90^0 whereas for E_y it is reverse i.e. E_y is minimum at 0^0 and maximum at 90^0. With the increase in volume fraction increase in E_x and E_y can be observed for a given fiber orientation. As the fiber alignment increases, decrease in E_x and increase in E_y can be observed. As per macromechanics based analytical study it is quite expected behavior. Considering the case when the fiber volume percentage (V_f) is 50 % (Fig. 11), E_x of the bamboo-PLA lamina is greater than that of other two laminas until the fiber orientation angle (θ) reaches 16^0. However, the jute-PLA lamina exhibits a greater longitudinal Young's modulus (E_x) than the remaining laminas from $\theta = 74^0$ forward. Between 16^0 and 74^0 E_x of flax-PLA lamina is greater than bamboo-PLA and jute-PLA laminas. E_x of bamboo-PLA lamina is more than jute-PLA lamina between 16^0 and 22^0, but from 22^0 onwards this behavior reverses and E_x of jute-PLA lamina is more than bamboo-PLA lamina. In case of E_y of lamina, it is maximum for jute-PLA lamina up to 16^0 and from 74^0 onwards it is maximum for bamboo-PLA lamina. Between 16^0 and 74^0 E_y is maximum for flax-PLA lamina and from 16^0 to 68^0 E_y of jute-PLA lamina is more than bamboo-PLA lamina but from 68^0 onwards it reverses and E_y of bamboo-PLA is more than jute-PLA lamina. But these angles for behavior of E_x and E_y is expected to change for the three laminas if fiber volume fraction is varied as shown in Figs. 18 and 19. From Fig. 18 in case of E_x it can be seen that up to fiber orientation of 20^0 bamboo-PLA lamina dominates followed by flax-PLA and jute-PLA laminae for 20 %, 40 % and 60 % fiber contents but for 80 % fiber content flax-PLA lamina dominates at all fiber orientation angle and bamboo-PLA lamina takes the lowest values after 10^0 fiber orientations. From Fig. 19 in case of E_y it can be seen that bamboo-PLA lamina dominates beyond 70^0 fiber orientation for all fiber contents.

From Figs. 3, 6 and 9 it can be observed that for all the given volume fractions, G_{xy} is maximum at 45^0 and with the increasing in volume fraction increase in G_{xy} can also be observed for all the three laminas which is expected behavior as per macromechanics of lamina. Of the three laminas G_{xy} is highest for bamboo-PLA lamina for all the volume fractions as shown in Fig. 20. For all the fiber contents and alignments G_{xy} is maximum for bamboo-PLA lamina followed by flax-PLA lamina and is minimum for jute-PLA lamina.

Similarly, Figs. 3, 6 and 9 show that ν_{xy} increases with increasing fiber alignment, reaches maximum and then decreases. The fiber alignment at which ν_{xy} reaches maximum are displayed in Table 6 for different fiber contents and the average fiber alignments for bamboo-PLA, flax-PLA and jute-PLA laminas at which maximum value of Poisson's is obtained are 29^0, 28^0 and 35^0 respectively. It can be observed that jute fibers need more orientation to obtain highest Poisson's ratio. In case of fiber content of 50 % (Figs. 14 and 15), the ν_{xy} of flax-PLA lamina is more than other two laminas for the fiber alignments up to 20.3^0 and beyond 36.6^0. For the fiber alignments between 20.3^0 and 36.6^0 bamboo-PLA is more than other two laminas as highlighted in Fig. 15. Also, the ν_{xy} of bamboo-PLA lamina is more than jute-PLA lamina up to the fiber alignment of 72.3^0 and beyond this angle ν_{xy} of jute-PLA lamina is more than bamboo-PLA lamina. But this behavior of

ν_{xy} is expected to change for the three laminas if fiber volume fraction is varied as shown in Fig. 21.

Figs. 4, 7 and 10 show that lamina level shear coupling coefficients $\eta_{xy,x}$ and $\eta_{xy,y}$ increase with increasing fiber alignment, reaches maximum and then decreases. The fiber alignment at which $\eta_{xy,x}$ and $\eta_{xy,y}$ reach maximum are shown in Table 6 for different volume fractions. At average fiber alignments of 22^0, 29^0 and 32^0 maximum value of $\eta_{xy,x}$ is obtained for bamboo-PLA, flax-PLA and jute-PLA laminas respectively and it highlights that bamboo fibers need less alignment to obtain maximum shear coupling coefficient when force is applied only in longitudinal direction. Whereas, to obtain maximum $\eta_{xy,y}$ the average fiber alignments are 68^0, 61^0 and 59^0 for BPL, FPL and JPL respectively and it shows that bamboo fibers need more orientation to get maximum value of shear coupling coefficient when force is applied only in transverse direction. For all volume fractions, at fiber orientation of around 60^0 onwards the values $\eta_{xy,x}$ decreases at the same rate whereas for $\eta_{xy,y}$ the values increase at same rate up to the fiber orientation of 30^0 and beyond 30^0 the values reach maximum at different rate depending on the fiber content. When it comes to the fiber percentage of 50 % (Figs. 15 and 16), $\eta_{xy,x}$ and $\eta_{xy,y}$ of bamboo-PLA lamina is higher than other two laminas for all the fiber alignments. The maximum value of $\eta_{xy,x}$ for bamboo-PLA, flax-PLA and jute-PLA laminas are obtained at fiber orientation angles 20^0, 25^0 and 29^0 respectively. Similarly, the maximum value of $\eta_{xy,y}$ for bamboo-PLA, flax-PLA and jute-PLA laminas are obtained at fiber orientations 70^0, 65^0 and 61^0 respectively. However, this behavior of $\eta_{xy,x}$ and $\eta_{xy,y}$ changes for the three laminas if fiber volume fraction is varied as shown in Figs. 22 and 23. For all the fiber contents and alignments $\eta_{xy,x}$ and $\eta_{xy,y}$ is maximum for bamboo-PLA lamina followed by flax-PLA lamina and is minimum for jute-PLA lamina.

The data on the variations of engineering constants with fiber orientation angle for various volume fractions will be very helpful in understanding the behavior of lamina and will make the process of designing a laminate based on the failure theories easier. The engineering constants of lamina are difficult to determine through single-layer studies, necessitating complex experimental setups due to the thin nature of lamina. Not only will it be unnecessary to perform experiments on a single lamina, but the approach based on the macro-mechanics of lamina for the calculation of E_x, E_y, G_{xy}, ν_{xy}, $\eta_{xy,x}$, and $\eta_{xy,y}$ of single lamina will also help to validate the experimental results of a lamina. Many such comparable findings can be drawn from the data pertaining to the engineering constants of lamina at different fiber content and orientation. Furthermore, advanced macro and micro-mechanical models can be used to study the effect of volume fraction on engineering constants. The study presented is purely theoretical and need to be validated experimentally, because it has not considered some practical issues like fiber matrix bonding strength and water absorption nature of bamboo fibers. There can be some challenges with the extraction of bamboo fibers and reinforcing natural fibers in the PLA matrix. The extraction of bamboo fibers is not as economical as that of the jute and flax fibers because the extraction of jute and flax fibers is standardized and is well practiced. In case of bamboo fibers extraction their challenges are associated with bamboo fiber length which is very small to handle and bamboo fibers can be extracted in many forms as single fiber, bundle of fibers and in strip form. And the usage of PLA as matrix is not as well spread as epoxy resin which is widely used and has well established market.

5.1. Conclusion

For all the three natural fiber-PLA laminae studied E_x is maximum at 0^0 and minimum at 90^0, E_y is minimum at 0^0 and maximum at 90^0, G_{xy} is increases reaches maximum at 45^0 and then decreases to zero at 0^0 and 90^0, ν_{xy} increases reaches maximum at certain angle and then decreases and similar behavior can be observed for $\eta_{xy,x}$, and $\eta_{xy,y}$. To obtain maximum E_x below 20^0 fiber orientation bamboo-PLA lamina can be used for all fiber contents and the same can be followed for E_y. Overall it can be concluded that, for all the fiber orientations and contents bamboo-PLA lamina gives desired engineering constants compared to flax-PLA and jute-PLA laminae. Selecting the appropriate staking sequence to design a natural fiber laminate made of hybrid green composite material is made easier by the variations of the engineering constants E_x, E_y, G_{xy}, ν_{xy}, $\eta_{xy,x}$, and $\eta_{xy,y}$ of the three natural fiber PLA lamina with the fiber orientation angle (θ) for different fiber volume fraction (V_f) presented in this paper. The study presented makes it easier to design a hybrid composite lamina based on PLA strengthened by reinforcing natural fibers bamboo, flax and jute. It not only helps in selecting proper fiber orientations for the three natural fibers but also to choose right fiber contents to get desired engineering constants. The approach and outcomes provided for the bamboo, flax and jute natural fibers will assist the researchers in selecting a natural fiber/s for the design of face sheets for the sandwich composite structures and in design of hybrid laminates reinforced with natural fibers in a biodegradable matrix for various purposes. The study presented in this paper need to be validated using experimental studies. The only practical difficulty that can be faced during experimental studies is with the bamboo fiber extractions.

CRediT authorship contribution statement

B. Vishwash: Writing – review & editing, Writing – original draft, Methodology, Investigation, Funding acquisition, Formal analysis, Data curation, Conceptualization. **N.D. Shivakumar:** Supervision, Resources. **K.B. Sachidananda:** Writing – review & editing, Resources.

Data availability

The research reported in this article did not involve the use of any data.

Declaration of competing interest

The authors declare that they have no known competing financial interests or personal relationships that could have appeared to influence the work reported in this paper.

Acknowledgement

The corresponding author Mr. B Vishwash would like to thank All India Council for Technical Education (AICTE), Government of India for providing scholarship to pursue Ph.D. at Indian Institute of Science, Bangalore under Quality Improvement Programme (QIP). Also, the corresponding author Mr. B Vishwash would like to thank the management of Siddaganga Institute of Technology, Tumakuru, Karnataka, India for providing study leave to pursue Ph.D. at Indian Institute of Science, Bangalore.

References

[1] Kiana Rafiee, Helge Schritt, Daniel Pleissner, Guneet Kaur, Satinder K. Brar, Biodegradable green composites: it's never too late to mend, Curr. Opin. Green Sustainable Chem. 30 (2021) 100482, https://doi.org/10.1016/j.cogsc.2021.100482. ISSN 2452-2236.

[2] F.P. La Mantia, M. Morreale, Green composites: a brief review, Compos. Appl. Sci. Manuf. 42 (6) (2011) 579–588, https://doi.org/10.1016/j.compositesa.2011.01.017. ISSN 1359-835X.

[3] Issam Elfaleh, Fethi Abbassi, Habibi Mohamed, Furqan Ahmad, Mohamed Guedri, Mondher Nasri, Christian Garnier, A comprehensive review of natural fibers and their composites: an eco-friendly alternative to conventional materials, Result. Eng. 19 (2023) 101271, https://doi.org/10.1016/j.rineng.2023.101271. ISSN 2590-1230.

[4] Y. Abhiram, Ashish Das, Keshav Kumar Sharma, Green composites for structural and non-structural applications: a review, Mater. Today: Proc. 44 (Part 1) (2021) 2658–2664, https://doi.org/10.1016/j.matpr.2020.12.678. ISSN 2214-7853.

[5] S. Sathees Kumar, P. Shyamala, Pravat Ranjan Pati, Jayant Giri, Emad Makki, T. Sathish, Mechanical (static and dynamic) characterization and thermal stability

of hybrid green composites for engineering applications, J. Mater. Res. Technol. 30 (2024) 7214–7227, https://doi.org/10.1016/j.jmrt.2024.05.132. ISSN 2238-7854.
[6] Dongping Yu, Ming Liu, Fuhao Xu, Yong Kong, Xiaodong Shen, Structure tailoring and thermal performances of water glass-derived silica aerogel composite with high specific surface area and enhanced thermal stability, J. Non-Cryst. Solids 630 (2024) 122889, https://doi.org/10.1016/j.jnoncrysol.2024.122889. ISSN 0022-3093.
[7] Lovisa Rova, Alia Gallet Pandellé, Zhenjin Wang, Hiroki Kurita, Fumio Narita, Japanese washi-paper-based green composites: fabrication, mechanical characterization, and evaluation of biodegradability, Compos. Appl. Sci. Manuf. 184 (2024) 108261, https://doi.org/10.1016/j.compositesa.2024.108261. ISSN 1359-835X.
[8] Shanshan Lv, Yanhua Zhang, Jiyou Gu, Haiyan Tan, Physicochemical evolutions of starch/poly (lactic acid) composite biodegraded in real soil, J. Environ. Manag. 228 (2018) 223–231, https://doi.org/10.1016/j.jenvman.2018.09.033. ISSN 0301-4797.
[9] W. Wang, M. Sain, P.A. Cooper, Study of moisture absorption in natural fiber plastic composites, Compos. Sci. Technol. 66 (Issues 3–4) (2006) 379–386, https://doi.org/10.1016/j.compscitech.2005.07.027. ISSN 0266-3538.
[10] Mouad Chakkour, Mohamed Ould Moussa, Ismail Khay, Mohamed Balli, Najma Laaroussi, Tarak Ben Zineb, Influence of fiber orientation on the moisture adsorption of continuous bamboo fiber composites, Mater. Today: Proc. (2023), https://doi.org/10.1016/j.matpr.2023.07.106. ISSN 2214-7853.
[11] Sujin Jose Arul, Priyabatra Adhikary, S.P. Jani, A. Haiter Lenin, Moisture diffusion analysis and their effects on the mechanical properties of organic particle filled natural fiber reinforced hybrid polymer composites, Int. J. Polym. Anal. Char. 29 (1) (2024) 42–55, https://doi.org/10.1080/1023666X.2023.2301271. ISSN 1023-666X.
[12] Bo Wu, Yu Wai Chung, Yihong Tang, Jishen Qiu, Effect of internal moisture content (IMC) on the CO2 sequestration efficiency of hollow natural fiber (HNF)-reinforced reactive magnesia cement (RMC) composites, Construct. Build. Mater. 428 (2024) 136339, https://doi.org/10.1016/j.conbuildmat.2024.136339. ISSN 0950-0618.
[13] Boxiang Zhan, Long Zhang, Yongqi Deng, Minghui Fan, Lifeng Yan, Sustainable adhesives for ultra-composites from biomass powder, Chem. Eng. J. 485 (2024) 149984, https://doi.org/10.1016/j.cej.2024.149984. ISSN 1385-8947.
[14] Y. Kondo, K. Miyazaki, K. Takayanagi, K. Sakurai, Surface treatment of PET fiber by EB-irradiation-induced graft polymerization and its effect on adhesion in natural rubber matrix, Eur. Polym. J. 44 (5) (2008) 1567–1576, https://doi.org/10.1016/j.eurpolymj.2008.02.020. ISSN 0014-3057.
[15] Sripathi Dev Sharma Kopparthy, Anil N. Netravali, Review: green composites for structural applications, Composites Part C: Open Access 6 (2021) 100169, https://doi.org/10.1016/j.jcomc.2021.100169. ISSN 2666-6820.
[16] Nasser A. Al-Tayyar, Ahmed M. Youssef, Rashad Al-hindi, Antimicrobial food packaging based on sustainable Bio-based materials for reducing foodborne Pathogens: a review, Food Chem. 310 (2020) 125915, https://doi.org/10.1016/j.foodchem.2019.125915. ISSN 0308-8146.
[17] Alok Kumar Trivedi, M.K. Gupta, Harinder Singh, PLA based biocomposites for sustainable products: a review, Adv. Industr. Eng. Polym. Res. 6 (4) (2023) 382–395, https://doi.org/10.1016/j.aiepr.2023.02.002. ISSN 2542-5048.
[18] Shady Farah, Daniel G. Anderson, Robert Langer, Physical and mechanical properties of PLA, and their functions in widespread applications—a comprehensive review, Adv. Drug Deliv. Rev. 107 (2016) 367–392, https://doi.org/10.1016/j.addr.2016.06.012. ISSN 0169-409X.
[19] S.N. Kasa, M.F. Omar, M.M.A.B. Abdullah, I.N. Ismail, S.S. Ting, S.C. Vac, P. Vizureanu, Effect of unmodified and modified nanocrystalline cellulose reinforced polylactic acid (PLA) polymer prepared by solvent casting method morphology, mechanical and thermal properties, Mater. Plast. 54 (1) (2017) 91–97, https://doi.org/10.37358/MP.17.1.4793.
[20] Thabang H. Mokhothu, Maya Jacob John, Review on hygroscopic aging of cellulose fibres and their biocomposites, Carbohydr. Polym. 131 (2015) 337–354, https://doi.org/10.1016/j.carbpol.2015.06.027. ISSN 0144-8617.
[21] Fabien Bogard, Thierry Bach, Boussad Abbes, Christophe Bliard, Chadi Maalouf, et al., A compara- tive review of Nettle and Ramie fiber and their use in biocomposites, particularly with a PLA matrix, J. Nat. Fibers (2021), https://doi.org/10.1080/15440478.2021.1961341.hal-03375929. https://hal.science/hal-03375929.
[22] Bo Madsen, Hans Lilholt, Physical and mechanical properties of unidirectional plant fibre composites—an evaluation of the influence of porosity, Compos. Sci. Technol. 63 (9) (2003) 1265–1272, https://doi.org/10.1016/S0266-3538(03)00097-6. ISSN 0266-3538.
[23] L. Donaldson, Microfibril angle: measurement, variation and relationships – a review, IAWA J. 29 (4) (2008) 345–386, https://doi.org/10.1163/22941932-90000192.
[24] Christian Bergfjord, Bodil Holst, A procedure for identifying textile bast fibres using microscopy: flax, nettle/ramie, hemp and jute, Ultramicroscopy 110 (9) (2010) 1192–1197, https://doi.org/10.1016/j.ultramic.2010.04.014. ISSN 0304-3991.
[25] Min Zhi Rong, et al., The effect of fiber treatment on the mechanical properties of unidirectional sisal-reinforced epoxy composites, Compos. Sci. Technol. 61 (10) (August 2001) 1437–1447, https://doi.org/10.1016/S0266-3538(01)00046-X.
[26] Sayyed Mahdi Hejazi, Mohammad Sheikhzadeh, Mahdi Abtahi Sayyed, Zadhoush Ali, A simple review of soil reinforcement by using natural and synthetic fibers, Construct. Build. Mater. 30 (2012) 100–116, https://doi.org/10.1016/j.conbuildmat.2011.11.045. ISSN 0950-0618.
[27] Akhtarul Islam Amjad, Bamboo fibre: a sustainable solution for textile manufacturing, Adv. Bamboo Sci. 7 (2024) 100088, https://doi.org/10.1016/j.bamboo.2024.100088. ISSN 2773-1391.
[28] Romi Sukmawan, Hitoshi Takagi, Antonio Norio Nakagaito, Strength evaluation of cross-ply green composite laminates reinforced by bamboo fiber, Compos. B Eng. 84 (2016) 9–16, https://doi.org/10.1016/j.compositesb.2015.08.072. ISSN 1359-8368.
[29] B.U. Kelkar, S.R. Shukla, P. Nagraik, B.N. Paul, Structural bamboo composites: a review of processing, factors affecting properties and recent advances, Adv. Bamboo Sci. 3 (2023) 100026, https://doi.org/10.1016/j.bamboo.2023.100026. ISSN 2773-1391.
[30] Md Yusof Fauziah, Nor 'Aini Wahab, Noor Leha Abdul Rahman, Anizah Kalam, Aidah Jumahat, Che Faridah Mat Taib, Properties of treated bamboo fiber reinforced tapioca starch biodegradable composite, Mater. Today: Proc. 16 (Part 4) (2019) 2367–2373, https://doi.org/10.1016/j.matpr.2019.06.140. ISSN 2214-7853.
[31] Lecoublet Morgan, Mehdi Khennache, Nathalie Leblanc, Ragoubi Mohamed, Christophe Poilâne, Physico-mechanical performances of flax fiber biobased composites: retting and process effects, Ind. Crop. Prod. 173 (2021) 114110, https://doi.org/10.1016/j.indcrop.2021.114110. ISSN 0926-6690.
[32] Libo Yan, Nawawi Chouw, Krishnan Jayaraman, Flax fibre and its composites – a review, Compos. B Eng. 56 (2014) 296–317, https://doi.org/10.1016/j.compositesb.2013.08.014. ISSN 1359-8368.
[33] S. Senthilrajan, N. Venkateshwaran, R. Giri, Sikiru O. Ismail, Rajini Nagarajan, Kumar Krishnan, Faruq Mohammad, Mechanical, vibration damping and acoustics characteristics of hybrid aloevera/jute/polyester composites, J. Mater. Res. Technol. 31 (2024) 2402–2413, https://doi.org/10.1016/j.jmrt.2024.06.158. ISSN 2238-7854.
[34] Morgane Tanguy, Alain Bourmaud, Johnny Beaugrand, Thierry Gaudry, Christophe Baley, Polypropylene reinforcement with flax or jute fibre; Influence of microstructure and constituents properties on the performance of composite, Compos. B Eng. 139 (2018) 64–74, https://doi.org/10.1016/j.compositesb.2017.11.061. ISSN 1359-8368.
[35] Nitish Kumar, Ramesh Kannan Kandasami, Surender Singh, Effective utilization of natural fibres (coir and jute) for sustainable low-volume rural road construction – a critical review, Construct. Build. Mater. 347 (2022) 128606, https://doi.org/10.1016/j.conbuildmat.2022.128606. ISSN 0950-0618.
[36] O. Das, N.K. Kim, D. Bhattacharyya, 16 - the mechanics of biocomposites, in: Luigi Ambrosio (Ed.), Woodhead Publishing Series in Biomaterials, Biomedical Composites, second ed., Woodhead Publishing, 2017, pp. 375–411, https://doi.org/10.1016/B978-0-08-100752-5.00017-2. ISBN 9780081007525.
[37] L. Nicolais, A. Gloria, L. Ambrosio, 17 - the mechanics of biocomposites, in: Luigi Ambrosio (Ed.), Woodhead Publishing Series in Biomaterials, Biomedical Composites, Woodhead Publishing, 2010, pp. 411–440, https://doi.org/10.1533/9781845697372.3.411. ISBN 9781845694364.
[38] Zheng-Ming Huang, Chapter One - mechanics theories for anisotropic or composite materials, in: Stéphane P.A. Bordas (Ed.), Advances in Applied Mechanics, vol. 56, Elsevier, 2023, pp. 1–137, https://doi.org/10.1016/bs.aams.2022.09.004. ISSN 0065-2156, ISBN 9780323992480.
[39] B. Vishwash, K.B. Sachidananda, N.D. Shivakumar, Examination of the implications of fibers' alignment and volume fraction on the engineering constants of natural fiber epoxy lamina using analytical research, Ind. Crop. Prod. 222 (Part 2) (2024) 119615, https://doi.org/10.1016/j.indcrop.2024.119615. ISSN 0926-6690.
[40] F.R. Cichocki Jr., J.L. Thomason, Thermoelastic anisotropy of a natural fiber, Compos. Sci. Technol. 62 (5) (2002) 669–678, https://doi.org/10.1016/S0266-3538(02)00011-8. ISSN 0266-3538.
[41] Paulo Peças, Hugo Carvalho, Hafiz Salman, Marco Leite, Natural fibre composites and their applications: a review, J. Composit. Sci. 2 (4) (2018) 66, https://doi.org/10.3390/jcs2040066.
[42] H. Lu, H. Lian, J. Xu, N. Ma, Z. Zhou, Y. Song, Y. Yu, X. Zhang, Study on the variation pattern and influencing factors of Poisson's ratio of bamboo, Front. Mater. 9 (2022) 896756, https://doi.org/10.3389/fmats.2022.896756.
[43] K.L. Pickering, M.G. Aruan Efendy, T.M. Le, A review of recent developments in natural fibre composites and their mechanical performance, Compos. Appl. Sci. Manuf. 83 (2016) 98–112, https://doi.org/10.1016/j.compositesa.2015.08.038. ISSN 1359-835X.
[44] Daniel Scida, Alain Bourmaud, Christophe Baley, Influence of the scattering of flax fibres properties on flax/epoxy woven ply stiffness, Mater. Des. 122 (2017) 136–145, https://doi.org/10.1016/j.matdes.2017.02.094. ISSN 0264-1275.
[45] V. Suthenthiraveerappa, V. Gopalan, Elastic constants of tapered laminated woven jute/epoxy and woven aloe/epoxy composites under the influence of porosity, J. Reinforc. Plast. Compos. 36 (19) (2017) 1453–1469, https://doi.org/10.1177/0731684417710108.
[46] F.R. Cichocki Jr., J.L. Thomason, Thermoelastic anisotropy of a natural fiber, Compos. Sci. Technol. 62 (5) (2002) 669–678, https://doi.org/10.1016/S0266-3538(02)00011-8. ISSN 0266-3538.
[47] V.C. Pinto, Tiago Ramos, Sofia Alves, J. Xavier, Paulo Tavares, P.M.G.P. Moreira, Rui miranda guedes, comparative failure analysis of PLA, PLA/GNP and PLA/CNT-COOH biodegradable nanocomposites thin films, Procedia Eng. 114 (2015) 635–642, https://doi.org/10.1016/j.proeng.2015.08.004. ISSN 1877-7058.